A new subfamily of ionotropic glutamate receptors unique to the echinoderms with putative sensory role

Rubaiyat E Sania*+, João C.R. Cardoso+, Bruno Louro, Nathalie Marquet, Adelino V.M. Canário*

CCMAR/CIMAR LA, Centro de Ciências do Mar do Algarve, Universidade do Algarve, Campus de Gambelas, 8005-139 Faro, Portugal

* Corresponding author:

Running title: Echinoderm Ionotropic Glutamate Receptors

+ Contributed equally.

Email addresses:
RS: a59583@ualg.pt
JCRC: jccardo@ualg.pt
BL: blouro@ualg.pt
NM: nmarquet@ualg.pt
AVMC: acanario@ualg.pt

Keywords: ionotropic glutamate receptors, phylogeny, echinoderms, sea cucumber, chemosensory receptors

Abstract

Chemosensation is a critical signalling process in animals and especially important in sea cucumbers, a group of ecologically and economically important marine echinoderms (Class Holothuroidea), which lack audio and visual organs and rely on chemical sensing for survival, feeding and reproduction. The ionotropic receptors are a recently identified family of chemosensory receptors in insects and other protostomes, related to ionotropic glutamate receptor family (iGluR) a large family of membrane receptors in metazoan. Here we characterize the echinoderm iGluR subunits and consider their possible role in chemical communication in sea cucumbers. Sequence similarity searches revealed that sea cucumbers have in general a higher number of iGluR subunits when compared to other echinoderms. Phylogenetic analysis and sequence comparisons revealed GluH as a specific iGluR subfamily present in all echinoderms. Homologues of the vertebrate GluA (*aka* α-amino-3-hydroxy-5-methyl-4-isoxazolepropionic acid, AMPA), GluK (*aka* kainate) and GluD (*aka* delta) were also identified. The GluN (*aka* N-methyl-d-aspartate, NMDA) as well as the invertebrate deuterostome subfamily GluF (*aka* phi) are absent in echinoderms. The echinoderm GluH subfamily shares conserved structural protein organization with vertebrate iGluRs and the ligand binding domain (LBD) is the most conserved region and genome analysis indicates evolution via lineage and species-specific tandem gene duplications. GluH genes (named Grih) are the most expressed iGluRs subunit genes in tissues in the sea cucumber *Holothuria arguinesis*, with *Griha1, Griha2 and Griha5* exclusively expressed in tentacles, making them candidates to have a chemosensory role in this species. The multiple GluH subunits may provide alternative receptor assembly combinations, thus expanding the functional possibilities and widening the range of compounds detected during aggregation and spawning in echinoderms.

Introduction

Chemosensation is an ancient sensory mechanism present from microbes to humans that allows the detection, processing, and response to information acquired from the environment (Yohe & Brand, 2018). In multicellular organisms, chemosensation occurs in specialized organs mediated by specific chemosensory receptors. The chemosensory receptors detect and discriminate the variety of chemical signals, which are translated into electrical signals to elicit specific behaviours such as food foraging, protection from predators, finding mates and other social behaviours (Bargmann, 2006; Kaupp, 2010). Most of the chemosensory receptors studied so far are members of the superfamily of seven transmembrane domain G protein-coupled receptor (GPCR), and include the odorant, gustatory and pheromone receptors (Bargmann, 2006; Touhara & Vosshall, 2009).

More recently, a group of chemosensory ionotropic receptors (IR), also with temperature sensing ability, and expressing in olfactory sensory neurons have been described in protostomes (insects, crustaceans and molluscs) (Benton et al., 2009; Croset et al., 2010; Ni et al., 2016; Rytz et al., 2013). The IRs are derived from the metazoan glutamate ionotropic receptors (iGluRs), an evolutionary well conserved family of ligand-gated ion channels that can assemble either as homo- or heterotetramers activated by glutamate that are best known for their role in synaptic communication in nervous systems (Traynelis et al., 2010; Twomey & Sobolevsky, 2018).The functional IR and iGluR are composed of several subunits sharing conserved structure and consisting of an extracellular amino-terminal domain (ATD) involved in subunit assembly, absent in some shorter IRs isoforms (Croset et al., 2010), a ligand-binding domain (LBD) followed by two transmembrane segments that form the ion pore channel, a third transmembrane domain and a cytosolic carboxy-terminal tail (Jin et al., 2009). The LBD domain is composed of two half-domains S1 and S2 that closes around glutamate (or related agonists) separated by the ion channel pore. iGluRs ligand selectivity for glutamine or related molecules depends on the residues within the LBD that regulate cation flow in response to an external chemical stimulus (Abuin et al., 2011; Karakas & Furukawa, 2014; Kumar et al., 2011; Ramos-Vicente et al., 2018; Traynelis et al., 2010). The protostome IRs differ from other iGluRs at the LBD as they lack the characteristic glutamate-interacting residues (Shepherd & Huganir, 2007; Wudick et al., 2018).

iGluRs are classified in four main subfamilies present in vertebrates and invertebrates and an official nomenclature (gene/protein) has been established (Collingridge et al., 2009): a-amino-3-hydroxy-5-methyl-4-isoxa-zolepropionic acid (AMPA) receptors (Gria/GluA), kainate receptors (Grik/GluK), N-methyl-D-aspartate (NMDA) receptors (Grin/GluN) and delta receptors (Grid/GluD). In invertebrates two other subfamilies are present: phi receptors (Grif/GluF), only described in deuterostomes (non-vertebrate chordates, hemichordates and echinoderms), and epsilon receptors (Grie/GluE), found in deuterostomes, in eumetazoans (Placozoa and Ctenophora) and cnidarians (Ramos-Vicente et al., 2018). In mammals, the 18 iGluR subunits are most expressed in neurones but they are also present in non-neuronal cells (Raible et al., 2006; Traynelis et al., 2010; Yelshanskaya et al., 2014). Epsilon receptors were found to be abundant in the amphioxus nervous system (Pascual-Anaya & D'Aniello, 2006) and form functional ligand-gated ion channels suggesting conserved structure and function with the vertebrate receptor sister subfamily (Ramos-Vicente et al., 2018).

Chemosensation is the prominent sense in the marine environment (Ache & Young, 2005; Giordano et al., 2017; Hardege & Bentley, 1997) and in benthic and slow-moving invertebrates such as echinoderms (Phylum Echinodermata), a large group of deuterostomes that lack vision and hearing organs, chemosensation is the major signalling mechanism for survival, feeding and reproduction (Hamel & Mercier, 1996, 1999; Marquet et al., 2018; Roberts et al., 2017). We have been using the sea cucumber, *Holothuria arguinensis* (Class Holothuroidea) as a model to understand echinoderm behaviour and reproduction. We have recently discovered that *H. arguinensis* males release odorants to attract other individuals to spawning aggregations and that at the time of spawning they release a pheromone that induces spawning in males and females (Marquet et al., 2018). Although the spawning pheromone has not been fully characterized it appears to include phosphatidylcholine derivatives (Marquet et al., 2018). However, the receptors and tissues involved in chemosensory detection in *H. arguinesis* still need to be identified, and how the signals are translated into behavioural and physiological actions is not yet understood. Sea cucumbers are ecological important bottom-dwelling marine echinoderms and as deposit feeders they play a fundamental role in nutrient recycling and restoration and biodiversity enhancement of the marine environment (Purcell et al., 2016). Overfishing is contributing to the decline of natural populations and understanding of their

reproductive behaviour and communication is essential for efficient fisheries management and to establish guidelines for aquaculture production (González-Wangüemert et al., 2016).

Echinoderms do not have a brain, and their simple central nervous system (CNS) consists of a circular nerve ring and radial nerve cords (Díaz-Balzac & García-Arrarás, 2018; Hoekstra et al., 2012). In sea cucumbers the nerve ring localizes at the base of tentacles, a highly sensory and enervated organ, from which radial nerves cords exit and enervate the body wall (Díaz-Balzac et al., 2010; Marquet et al., 2020; San Miguel-Ruiz et al., 2009). As a step towards identifying chemosensory neurones in sea cucumbers, we have mapped neurones that use nitric oxide and other signalling mechanisms in *H. arguinensis* (Marquet et al., 2020). We have also characterized the olfactory receptor-like (OR-like) GPCR repertoire and identified 79 in the *Apostichopus japonicus* genome and 57 in tissue transcriptomes of *H. arguinensis* (Marquet et al., 2020). The OR-like repertoire of *H. arguinesis* expresses mostly in tentacles, oral cavity and papillae/tegument and is smaller than in other echinoderms (*S. purpuratus* and *A. planci*) (Hall et al., 2017; Marquet et al., 2020; Raible et al., 2006; Roberts et al., 2017; Sea Urchin Genome Sequencing et al., 2006) suggesting that mediation and transmission of environmental chemical cues in echinoderms may be regulated by different molecular mechanisms.

Recently, two putative iGluRs subunits were described in *A. planci* (named gKAR2 and GluR2, orthologues of the vertebrate GluN and GluA, respectively) and their abundance in sensory tentacle suggested they could take part in chemosensation (Roberts et al., 2017). Here, we hypothesize that iGluRs could have a chemosensory role in sea cucumbers and characterize the iGluR subunit repertoire in sea cucumbers and other echinoderms using genomes and transcriptomes and a combination of sequence functional annotation and phylogenetic analyses. We found sea cucumbers and other echinoderms to possess a specific subfamily of iGluR subunits named GluH (with corresponding gene name Grih) in accordance to established convention for ligand-gated ion channels (Collingridge et al., 2009; Tweedie et al., 2021). No putative IR-like genes or transcripts were found in echinoderms as members of this subfamily were exclusively present in protostomes. The *H. arguinesis* iGluRs were mapped to the different tissue libraries to determine their primary expression location and abundance and infer potential roles in chemosensation. Grih genes were the most

abundant type with some exclusively expressed in tentacles highlighting their key role in the assembly of functional iGluRs that may be involved in echinoderm chemosensation.

Material and Methods

Ethical approval

H. arguinensis (class Holothuroidea, subclass Aspidochirotida) specimens were collected and handled in agreement with a license of the ICNF, Instituto da Conservação da Natureza e das Florestas, Portugal (License N° 635/2015/CAPT). This species is not endangered or protected.

Animals and tissue collection

H. arguinensis (> 210 mm length) were hand collected from the intertidal zone of the Ria Formosa (37°00′35.02″N; 7°59′46.10″O) in Faro (Portugal) and transported live in individual plastic bags filled with natural sea water to the laboratory. Sea cucumbers show no sexual dimorphism from external appearance. Sex and maturity stages were determined from gonadal biopsies and observation under light microscopy (LeicaDM2000). Adults, 5 females and 12 males, were used in the present study. Sea cucumbers were anesthetized by immersion in sea water with added $MgCl_2$ (5%), tissues were dissected out (tentacles, nerve ring, and radial nerve) and immediately frozen on dry ice and kept at −80 °C for RNA extraction.

RNA processing and sequencing

Total RNA was extracted from 40-45 mg of tissue using the E.Z.N.A. Total RNA Kit I (Omega Bio-Tek, USA) according to the manufacturer's instructions. Samples were treated with RNase-free DNase I (Omega Bio-Tek) to remove possible genomic DNA contamination. The integrity and quality of the extracted RNA was assessed by gel electrophoresis on a 0.8 % agarose 1x TBE gel. The RNA purity and quantity were determined on a NanoDrop One (Thermofisher, Spain). Sequencing library preparation and sequencing was conducted by Admera Health (New Jersey, USA) using a Illumina TrueSeq Stranded mRNA with Poly-A selection library kit (100- 500 ng RNA input) to generate 150 base paired-end reads (RNA-seq data have been deposited in the ArrayExpress database at EMBL-EBI under accession number E-MTAB-10369) (Canario, 2021).

Transcriptome Sequence assembly and annotation

Reference transcriptomes of tentacles, nerve ring and radial nerve from adult *H. arguinensis* were used to screen for iGluR transcripts. Quality control of raw reads and editing was performed with Trimgalore wrapper script v. 0.6.4 (Krueger, 2015) producing simple descriptive statistics and edited reads, before assembly. Tissue specific de novo assemblies were obtained using Trinity v. 2.10.0 with the default parameter and "–SS_lib_type RF" for stranded information of reads (Haas et al., 2013). The pair-end reads from each of the three tissue libraries were used to assemble tissue specific *de novo* transcriptomes (Supplementary Table 1). To evaluate the quality of the produced assembly, sequenced reads were mapped back to the reference assembly and quantitative and qualitative measures were applied using TransRate assembly and contig scores (Smith-Unna et al., 2016). Trinity scripts were used to quantify transcript abundance according to the Trinity quantification workflow (Grabherr et al., 2011). The *H. arguinensis* reference tissue transcriptomes were used as the scaffold for mapping and gene expression quantification. Mappings of reads to the reference assembled transcriptome was done using Bowtie 2 (Langmead & Salzberg, 2012). Calculation of abundance estimation values (counting) of the mapped reads was performed with RSEM (Li & Dewey, 2011), followed by EdgeR (Robinson et al., 2010) to identify significant gene expression variation. Levels of expression were quantified using fragments per kilobase of transcript per million mapped reads (FPKM). A three-way analysis of variance with sex, tissue and receptor as factors was used to compare differences in expression levels (FPKM), followed by the multicomparison Holm-Sidak a posteriori test when main effects were statistically significant. Statistical analysis was performed using SigmaPlot software (version 14.0, Systat Software, Inc).

Sequence database searches, alignments, and phylogenies

To identify the putative iGluRs in sea cucumber, an *in house* generated database of iGluR amino acid sequences (205) collected from vertebrates, invertebrate deuterostomes and protostomes was created. The dataset contained 18 *Homo sapiens* iGluR sequences obtained from ENSEMBL which were used as bait in protein BLAST queries (Altschul et al., 1990) to retrieve homologues from: 1) several chordates (phylum Chordata) - two vertebrates (subphylum Vertebrata) the ray-finned

fish spotted gar (*Lepisosteus oculatus*) and the cartilaginous fish elephant shark (*Callorhinchus milii*), the tunicate (subphylum Tunicata) sea squirt (*Ciona intestinalis*), the cephalochordate (subphylum Cephalochordata)amphioxus (*Branchiostoma lanceolatum*), 2) the hemichordate (phylum Hemichordata) acorn worm (*Saccoglossus kowalevskii*), 3) and several representatives of the phylum Echinodermata, the purple sea urchin (*Strongylocentrotus purpuratus*, Class Echinoidea), crown-of-thorns starfish (*Acanthaster planci*, Class Asteroidea), and the Japanese sea cucumber (*Apostichopus japonicus*, Class Holothuroidea); 4) several protostomes from the phylum Mollusca - the Pacific oyster (*Crassostrea gigas,* Class Bivalvia), a freshwater snail (*Biomphalaria glabrata,* Class Gastropoda), the California sea hare (*Aplysia californica,* Class Gastropoda) and the California two-spot octopus (*Octopus bimaculoides*, Class Cephalopoda) – and from the phylum Insecta the fruit fly (*D. melanogaster*) IR8a and IR25a linked to chemosensation (Croset et al., 2010). To be as comprehensive as possible the sequences from the recently published study by Ramos-Vicente et al. (2018) and those available at the National Center for Biotechnology Information (NCBI) were included. To enrich the echinoderm data we used receptor sequences of the different holothurian receptor subfamilies (GluH, GluA, GluK, GluD) as well as starfish GluN, cephalochordate GluF, insect *D. melanogaster* IR25a to search publicly available genome and protein data from two starfishes the crown-of-throne starfish (*Asterias rubens*) and European starfish (*Patiria miniata*), two sea urchins, the green sea urchin (*Lytechinus variegatus*) and the slate pencil urchin (*Eucidaris tribuloides*), two sea cucumbers, the brown mottled sea cucumber (*Australostichopus mollis*) and the brown sea cucumber (*Actinopyga echinites*), and from the Class Ophiuroidea, the brittle star (*Ophionereis fasciata*) and the sea lily (*Anneissia japonica*, Class Crinoidea). All searches were performed against the most recent annotated assemblies available from ENSEMBL and NCBI (Supplementary Table 2).

De novo assembled sea cucumber *H. arguinensis* tissue transcriptomes were searched separately using stand-alone translated nucleotide BLAST (tblastn) queries against the in-house iGluR database with an e-value cut-off of e^{-25}. The retrieved nucleotide sequences were translated to amino acids and confirmation as putative iGluR was confirmed using protein BLAST searches against the human (taxid:9605) non-redundant protein sequences (nr) database at NCBI. When identical transcripts

were retrieved from the transcriptome the longest was reserved and partial duplicates deleted from the analysis. To identify unique transcripts and account for potential sequencing errors the predicted proteins were clustered using CD-HIT v4.8.1 (Li & Godzik, 2006) and sequences > 97% amino acid identity were considered to be from the same transcript.

Sequence comparisons and phylogenetic analysis

Multiple sequence alignments of deduced iGluRs proteins were performed using the MUSCLE algorithm in Aliview v1.22 (Larsson, 2014) and conserved regions identified. The percentage of amino acid sequence identity/similarity was calculated with GeneDoc v2.7 (Nicholas & Nicholas, 1997). Protein domains were identified using Pfam v33.1 (Mistry et al., 2021) and from alignments with the *B. glabrata* homologues following Liang et al. (2016). The transmembrane domain regions and the signal peptide domain were predicted using the TMHMM Server v.2.0 (Krogh et al., 2001) and SignalP-5.0 (Almagro Armenteros et al., 2019). For the phylogenetic analysis, incomplete sequences and major sequence gaps were removed from the protein alignment. Trees were constructed using the VT model that best fitted the data given by model test-ng 0.1.5 in the CIPRES Science Gateway v3.3 (Miller et al., 2010). The Bayesian Inference (BI) tree was built using MrBayes (Ronquist et al., 2012) on XSEDE v3.2.7a (Towns et al., 2014) and 1.000.000 generation sampling and probability values to support tree branching. The maximum likelihood (ML) trees were built with the RAxML v8.2.12 method with 1000 bootstrap replicates (Stamatakis, 2014). Both trees were rooted using the *Arabidopsis thaliana* receptors Ath_GLR2 (NP_180476.3) and Ath_GLR5 (NP_565744.1) (Ramos-Vicente et al., 2018), visualized on FigTree v1.4.4 (Rambaut, 2016) and edited in Inkscape v0.92.3.

Nomenclature

The iGluRs are a large and extensive family of genes with different receptors subtypes in metazoans. In the present study, we followed the adopted nomenclature by the International Union of Pharmacology Committee on Receptor Nomenclature and Drug Classification (Collingridge et al., 2009) and the gene symbol from the *H. sapiens* gene nomenclature committee (Tweedie et al., 2021) summarized in Table 2. Accordingly, we have renamed the cephalochordate-specific epsilon and phi

receptors. The newly identified echinoderm iGluR subfamily reported in this study was designated as Grih (gene/transcripts) and GluH (proteins). Members that clustered clustering with the vertebrate canonical subfamilies were named following Ramos-Vicente et al. (2018). Paralogues from the other subfamilies were randomly numbered.

Gene neighbourhood analysis

The predicted protein sequences of a maximum of 10 neighbouring genes upstream and downstream of the iGluR encoding genes were retrieved from the *A. japonicus* genome ASM275485v1 at NCBI and used to query the genomes of *S. purpuratus* (Spur_5.0, GCA_000002235), *A. planci* (assembly OKI-Apl_1.0), *H. sapiens* (GRCh38.p13 (GCA_000001405.28), *L. oculatus* LepOcu1 (GCA_000242695.1) tunicate (KH (GCA_000224145.1), *B. lanceolatus* (BraLan2, GCA_900088365) and *C. gigas* (oyster_v9, GCA_000297895.1). The identity of the genes with hits for the *A. japonicus* homologues was confirmed by retrieving their sequences and reverse search on *A. japonicus* genome assembly. No syntenic regions were found in the *C. gigas*, *B. lanceolatu*s and *C. intestinalis* genomes.

Quantitative polymerase chain reaction

Three hundred ng of DNase-treated total RNA (denatured at 65℃) from the same samples used for sequencing (from tentacles, nerve ring and radial nerve), were used to synthesize cDNA in a final reaction volume of 20 µL with 200 ng of random hexamers (Jena Biosciences, Germany), 10 mM dNTPs (Promega, USA), 100 U RevertAid Reverse Transcriptase (RT, Promega) and 8 U of Ribolock RNase Inhibitor (ThermoFisher) incubating for 10 min at 20 ℃; 50 min at 42 ℃ and 5 min at 72 ℃. cDNA integrity and quality were assessed by amplifying the *18S* ribosomal RNA.
Quantitative reversed transcription-polymerase chain reaction (qPCR) was used to confirm expression of four of the most abundant transcripts *Griha5*, *Grihb*, *Grihc1* and *Grihc2* in male *H. arguinensis* cDNAs (n = 3). Specific primer pairs for each transcript with amplicon sizes between 116 and 189 base pairs were designed using primer-BLAST (Ye et al., 2012) at the NCBI (Table 1). qPCR reactions were performed on a CFX ConnectTM Real-TIME PCR Detection System (Bio-Rad, Portugal) using 96-well micro plates (Axygen) and products were sequenced to confirm their identity. Reactions were performed in duplicate in a final volume of 10 µl containing 2 µl of 1:10

and 1:5000 diluted cDNA for target genes and *18S*, respectively, SsoFast EvaGreen Supermix (Bio-Rad) and 300 nM of the forward and reverse specific primer. Optimized conditions consisted of 95 °C for 30 s, followed by 45 cycles of 95 °C for 5 s and 10 s at the appropriate annealing temperature for primers. Melting curves were performed to detect nonspecific products and primer dimers and target specificity was confirmed by the presence of a single peak in each melt curve. Standard curves were prepared from serial dilutions of quantified amplicons. Control reactions were included in all runs to confirm the absence of genomic DNA. qPCR reaction efficiencies were between 88.0 – 92.6% and the coefficient of determination $r^2 > 0.99\%$ for each target transcript. Gene expression was normalized to *18S*.

Results

The echinoderm ionotropic glutamate receptors

BLAST searches found 15 iGluR subunit transcripts in the tissue libraries of *H. arguinensis*, 18 genes in the *A. japonicus* genome (Figure 1) and at least 8 and 5 genes, respectively, in the *A. mollis* and *A. echinites* incomplete genome assemblies. In the sea urchin, iGluR subunit genes varied from 10 in *S. purpuratus* to 11 in *L. variegatus* and a similar number seem to exist in the starfishes (10 in *A. planci* and 9 in *P. miniate*) (Figure 1). In the crinoids, iGluR subunit genes varied between 10 in *A. japonica genome* and 6 in *O. fasciata*.

Phylogenetic analysis identifies a new subfamily unique to the Echinodermata which was named GluH and is the most gene rich within this phylum (Figures 1 and 2). Our BI and ML phylogenetic analysis support that the unique echinoderm GluH cluster with GluF and protostome IRs and are closely related to the metazoan GluK and GluA (Figure 2A and B). The GluN was the first metazoan receptor lineage to diverge, and our analysis support a close evolutionary proximity between the protostome IR8a/25a with the metazoan GluD (Figure 2A). No homologs to protostome IR genes were retrieved from any of the echinoderms or other deuterostomes, confirming they are specific to this group (Figure 2B).

The GluH subfamily is composed of 3 main receptor clades, GluHA, GluHB and GluHC, containing receptor sequences from the twelve echinoderms studied. Clustering of the different sequences suggests they resulted from lineage and species-specific duplications (Figure 2B). The other echinoderm iGluR family members cluster

with the vertebrate homologues. The echinoderm GluA and GluK sequences form a distinct cluster with two branches suggesting that they duplicated prior to the echinoderm radiation (Figure 2B).

Homologues of the GluD family were also found but a single gene was present in the echinoderms (Figure 2B). No members of the GluN subfamily were identified in the Holothuridea and Echinoidea lineages, although members were found among the Asteroidea and the Crinoidea, suggesting an ancestral Grin gene was deleted in the Echinozoa lineage (Figure 2B). Except for two GluE in the Crinoidea, no homologues of the recently described GluE were identified in echinoderms. GluF is specific to cephalochordates, IR is only found in protostomes and both subfamilies cluster with GluH, suggesting these subfamilies only persisted in invertebrate genomes and are restricted to these taxa.

Sequence comparisons and protein domain characterization

The structural features of the echinoderm iGluR subunits are conserved with those of vertebrate with few exceptions (Figure 3). For some of the echinoderm GluH, GluA and GluK no signal peptide was predicted suggesting different cellular localization. An extra transmembrane domain localized at the protein N-terminus was predicted for some of the echinoderm GluH and GluA members suggesting that they may have different architectures. The single echinoderm GluD possesses the LBD and the C-terminal (CTD) domains, but the incomplete sequence does not allow confirmation of the presence of the ATD region (Figure 3, Supplementary Figures 3, 4 and 5).

The ATD and CTD are the least conserved regions and the S1 and S2 domains within the LBD are the most conserved. The S1 and S2 of the GluH receptors share only 39-46% amino acid sequence similarity with the vertebrate orthologs suggesting that they may be activated by different molecules. The higher amino acid sequence conservation between the echinoderm GluA (S1, 57-74% and S2 56-69%) and GluK (S1, 71-83% and S2 72-77%) and the homologue regions in vertebrates revealed that they are probably activated by similar ligands (Figure 3).

iGluR activation is associated with the binding of glutamate or other amino acids (glycine, D-serine, aspartate and glutamate analogues) to the LBD. Arginine (R) localized within S1 domain and threonine (T) and aspartic acid/glutamic acid (D/E) within S2 are important conserved amino acid interacting residues (Armstrong et al., 1998; Stroebel & Paoletti, 2020). In sea cucumbers, the deduced iGluR (GluA, GluK

and GluD) proteins revealed that the R is fully conserved, but this is not the case for the other two residues (Figure 4). The overall conservation of the functional positions suggests that the sea cucumber receptors are likely to be activated also by amino acids but not necessarily the same.

Short-range gene environment conservation

The gene environment of the sea cucumber iGluR subunit genes was characterized to better understand receptor gene family evolution and the origin of the newly identified GluH subfamily (Figure 5, 6 and 7). In *A. japonicus*, the 11 newly identified Grih genes are distributed in four genome regions and gene arrangement within each region suggests that they resulted from tandem duplication events (Figure 5). Similarly, a highly homologue region was found in the *S. purpuratus* genome where the five Grih genes are also arranged in tandem. In *A. japonicus*, the remaining Grih genes are dispersed in pairs in three other genome regions and identification of duplicate *Slc3a1* neighbour suggests that the genome regions that encode for *Grihc6* and *Grihc4* (MRZ01001152.1), and *Grihc7* and *Grihc5* (MRZV01001222.1) resulted from a species-specific duplication. This explains the highest sequence similarity between the *Grihc6* and *Grihc7*, and *Grihc4* and *Grihc5* sequences. In *S. purpuratus* a single genome region that encodes for the orthologues of the *A. japonicus* gene neighbours of *Grihc6* and *Grihc4* and *Grihc7* and *Grihc5* was also identified, but no Grih gene was found there. This suggests that after the divergence of the two classes of echinoderms, gene duplications and gene translocation occurred in the *A. japonicus* genome. In *A. planci*, three Grih genes also map in tandem in the same genome fragment (NW_019091545.1) (Figure 5). In vertebrates no GluH homologue exists but in *L. oculatus* genes in linkage were found mapping in proximity, in chromosomes that contain Grin and Grik genes, providing evidence for a common origin between GluH and vertebrate iGluR subfamilies.

The *A. japonicus* Grik and Gria genes are differently arranged in the genome, and they share conserved gene linkage with the other echinoderm and vertebrate genome regions that encode the subfamily members (Figure 6 and 7A). In *S. purpuratus* and *A. planci*, the two Grik and the two Gria genes map in tandem, suggesting that receptors evolved under different pressure in echinoderms. For the echinoderm Grid genome regions, a conserved gene environment was found between *A. japonicus* and *S. purpuratus* but no homolog genome region was detected within the *A. planci* Grid

411 locus or in vertebrates (Figure 7B). Curiously, in all *A. japonicus*, *S. purpuratus* and *A.*
412 *planci* the Gria genes are flanked by the ionotropic GABBA receptors (*gabrb3* and
413 *gabbr2*) and in *L. oculatus* LG7, *gria4a* and *gabrb3* also map in proximity (Figure 7A).
414

415 **Expression of iGluR gene subunits in *H. arguinensis***

416 Quantification of iGluR subunit transcripts in the tissue libraries of *H. arguinensis*
417 (Figure 8) found Grih genes to be the highly expressed in the three tissue
418 transcriptomes. *Grihb*, *Grihc1* and *Grihc2* are the most abundant across the 3 tissue
419 libraries. The expression profile between males and females is generally similar but
420 levels of expression tend to be higher in females for some genes and tissues (Figure
421 8). *Griha1, Griha2*, *Griha5* and *Grik* seem to be specific to the tentacle, while *Griha4*
422 and *Grihc3* appear specific to the radial nerve (Figure 8). qPCR of the most abundant
423 genes, confirmed expression of *Grihb*, *Grihc1* and *Grihc2* in tentacles, nerve ring and
424 radial nerve of male *H. arguinesis* (Supplementary Figure 5).

425 # Discussion

426 We identified GluH, a novel iGluR subfamily exclusively found in echinoderms. GluH
427 is also the most expanded and diverse echinoderm iGluR subfamily and has evolved
428 by lineage and species-specific gene duplications. It is also largely expanded in sea
429 cucumbers compared to sea urchins and sea stars. Homologues of the canonical
430 GluA, GluK and GluD subfamilies are also present in echinoderms, but GluN was
431 absent from the Holothuridea and Echinoidea lineages. Primary structure analyses
432 suggest functional divergence of the GluH from other iGluRs. The high expression of
433 specific isoforms in sensory tissues in *H. arguinensis* suggest they may play an
434 important role in neuronal transmission and abundance in tentacles indicate they are
435 novel targets to unravel chemosensation in sea cucumbers and possibly all
436 echinoderms.

437 **GluH, a novel iGluR subfamily specific to echinoderms**

438 GluH is a novel iGluR subfamily, which our extensive phylogeny places exclusively
439 with the echinoderms. This contrasts with a recent report which, based on a more
440 limited number of sequences, clustered the echinoderm iGluR with members of the
441 cephalochordate and hemichordate GluF (Ramos-Vicente et al., 2018). The GluF

subfamily was suggested to have been lost in the lineages of protostomes, urochordates and vertebrates (Ramos-Vicente et al., 2018) and our analysis indicate that it is only present in cephalochordates. GluF was also previously suggested to exist in hemichordates, but our analysis failed to cluster the hemichordate sequence with any of the clades. In our evolutionary analysis, which included data from 12 echinoderms, GluH clusters in the same tree branches as the cephalochordate GluF and mollusc IR, indicating shared origin of a group of invertebrate specific iGluRs/IRs and pointing to shared conservation of physiological roles in different taxa.

The GluH subfamily is not closely related to the canonical vertebrate iGluR members (GluA, GluK, GluN and GluD) but they share a common origin and possess a similar protein modular structural organization with an extracellular N-terminal, bipartite ligand binding domain and short cytoplasmic C/terminus (Mayer et al., 2006). In the class Holothuroidea, as revealed by the members found in the *A. japonicus* genome and *H. arguinensis* tissue transcriptomes, GluH/Gri members expanded when compared to other echinoderms and considering their position in the *A. japonicus* genome as tandem gene arrays (from 2 to 5 genes) in different chromosome fragments. Moreover, three types of Grih genes exist (*Griha, Grihb* and *Grihc*) that resulted from gene duplication events early during the echinoderm radiation. Differences between types in the threonine (T) residue localized in the first half of the S2 domain that contacts the glutamate γ-carboxyl group suggest that they may have different amino acid affinities (Abuin et al., 2011; Chen et al., 2004). The sea cucumber GluHA possesses the conserved T residue in the S domain (Mayer et al., 2006; Naur et al., 2007). In GluHB, this T residue was mutated to alanine (A), a mutation that had no effect on localization or function of IR8a (Abuin et al., 2011) but reduced glutamate potency by three orders of magnitude in the NR2A subunit of NMDA (GluN) receptors (Anson et al., 1998; Chen et al., 2004). Most of GluHC threonine position in S2 was modified to serine (S), maintaining polarity and likely ligand characteristics. In addition, an extra transmembrane region localized in the ectodomain was predicted for *H. arguinensis* GluHC2 and GluHC3 and for *S. purpuratus* GluHC1, suggesting that they may have a different conformation in the cell membrane and thus potential modified function.

The GluN subfamily is absent from sea cucumber and sea urchin genomes

The sea cucumber GluA, GluK and GluD homologues have high similarity to their vertebrate orthologs and the high conservation in the LBD suggests that may have similar function. The apparent absence of GluN in sea cucumbers and sea urchins is intriguing, as members are found in starfish as well as in the crinoids. In vertebrates, GluN members are critical for the development of the central nervous system (CNS), generation of breathing and locomotion rhythms, and the processes underlying learning, memory, and neuroplasticity (Baez et al., 2018; Hansen et al., 2017). Evolutionary analysis performed by us and others (Ramos-Vicente et al., 2018) suggest that GluN was the first iGluR subfamily to diverge which subsequently duplicated originating three types in vertebrates, GluN1, GluN2 and GluN3. Homologues of the three GluN types are also present in invertebrates suggesting that duplication of an ancestral *Grin* gene in the different members occurred early in evolution (Ramos-Vicente et al., 2018). The absence of GluN homologues from 7 representatives of the Echinozoa lineage makes it unlikely to be a consequence of incomplete genome assemblies and suggests that the genes were subsequent deleted in this lineage. Their role in echinoderm physiology remains to be established.

A putative chemosensory role for GluH

We have previously found that sea cucumbers maintained a reduced number of GPCR olfactory-like receptors (OR) when compared to other echinoderms (Marquet et al., 2020). In *H. arguinesis* and in *A. japonicus*, 4 OR types were found (totalling 57 and 79 ORs, respectively) from an assembly of sensory and reproductive tissues, compared to around 300 identified in *A. planci* and *S. purpuratus* (Marquet et al., 2020). The iGluR repertoire in *H. arguinesis*, *A. japonicus*, and other echinoderm genomes, is much smaller than ORs, and gene number is relatively well conserved, albeit expanded in *H. arguinesis* and *A. japonicus*. Gene duplication is a fundamental process in evolution and a major source of protein functional diversity and adaptive innovations (Guschanski et al., 2017). In eukaryotes tandem gene duplication is one of the main gene mechanisms of gene evolution and sources of genetic novelty and tandem gene expression is regulated by the same elements (Lan & Pritchard, 2016). The *A. japonicus* iGluRs and ORs possess a similar genome rearrangement and most genes resulted from tandem gene duplications. We hypothesised these were probably associated to species-specific adaptations fuelled by their natural environment to

detect and transduce the signal of specific sensory (mostly chemosensory) cues (Marquet et al., 2020).

Families of chemoreceptor genes are suggested to have evolved independently across distinct phyla as a consequence of species-specific physiology and behaviour (Ache & Young, 2005). A key feature of chemoreceptors is their expression in sensory organs and in many protostome invertebrates IR expression patterns indicate that they are a group of ancestral receptors that are exclusively expressed or are clearly enriched in chemosensory organs/tissues, such as in insects, crustaceans and molluscs (Benton et al., 2009; Corey et al., 2013; Croset et al., 2010; Groh-Lunow et al., 2015; Liang et al., 2016; Liu et al., 2010; Olivier et al., 2011; Stepanyan et al., 2004). In *D. melanogaster*, IRs largely expanded in the genome due to species-specific homologous recombination and retroposition and increased gene number was suggested to improve the detection of different chemosensory signals (Croset et al., 2010). In that species, a few IRs have been suggested to be olfactory receptors and functional studies revealed that IRs can be activated by odours. The majority of non-olfactory IRs are expressed in peripheral and internal organs such as gustatory neurons and involved in other sensory functions such as taste (Croset et al., 2010; Rytz et al., 2013; Silbering et al., 2011). IR25a and IR8a were the first type of IRs associated to chemosensation and they show conserved expression in several protostome olfactory organs (Croset et al., 2010; Liu et al., 2010; Olivier et al., 2011; Stepanyan et al., 2004). Although absent from echinoderms, IRs are evolutionary related to other metazoan iGluRs suggestive of potentially conserved functional overlapping (Croset et al., 2010; Roberts et al., 2018). In echinoderms, the tentacles are important enervated and sensory organ appendages that allow echinoderms to move or to handle food (Cameron & Fankboner, 1984; Díaz-Balzac et al., 2010; Hamel & Mercier, 2011) and expression of two members homologues of vertebrate GluR2 (our GluA) and gKAR2 (our GluD) in the tentacles and tube feet of *A. planci* was taken to suggest involvement in chemosensation (Roberts et al., 2018). Interestingly, tentacles of both males and females *H. arguinensis* strongly and exclusively expressed a group of *Grih* subunit genes, and the the expression level of iGluR genes in this tissue is orders of magnitude higher compared to the olfactory receptor-like GPCRs expressed in the same tissue (Marquet et al., 2020). This suggests that one

538 or more GluH members are candidate (chemo)sensory receptors in *H. arguinensis*
539 and possibly other echinoderms.

540 **Conclusions**

541 The iGluR is an ancient receptor family with important functions in the nervous
542 and sensory system of metazoans, which has undergone specific gene expansions
543 and deletions. This led to some subfamilies being exclusive of certain taxa, possibly
544 activated by different ligands, implying specific adaptations. GluH is a novel subfamily
545 of iGluR highly expanded and unique to echinoderms. The abundant expression of
546 different GluH subunit receptor isoforms in sea cucumber sensory (tentacles) and
547 neuroregulatory tissues (radial nerve and the nerve ring) suggest they may participate
548 in the assembly of different types of iGluR complexes. The multiple GluH subunits may
549 provide alternative receptor assembly combinations, thus expanding the functional
550 possibilities and widening the range of compounds detected. Future studies will aim
551 at deorphanizing GluH receptors and establishing the biochemical and physiological
552 mechanisms behind chemosensory responses during aggregation and spawning in
553 sea cucumbers.

554 **Author contributions**

555 AVMC and JCRC conceived the study; RES and NM collected tissues; RES extracted
556 RNA and performed qPCR; RES, BL and JCRC analysed the data; RES and JCRC
557 wrote the first draft. All authors critically read and revised the manuscript.

558 **Data availability**

559 The sequence read data and sample information from this study were deposited in
560 ArrayExpress and can be accessed through the following ArrayExpress accession: E-
561 MTAB-10369. The datasets analysed in this study are publicly available and the
562 sources are referenced in the text.

563 **Acknowledgements**

564 This study was funded by Portuguese Foundation for Science and Technology (FCT)
565 through project UIDB/04326/2020. BL was supported by FCT under “Norma
566 transitória” contract DL57/2016/CP1361/CT0005 with Universidade do Algarve.

567 **References**

568 Abuin, L., Bargeton, B., Ulbrich, M. H., Isacoff, E. Y., Kellenberger, S., & Benton, R.
569 (2011). Functional architecture of olfactory ionotropic glutamate receptors.
570 *Neuron*, *69*(1), 44–60. https://doi.org/10.1016/j.neuron.2010.11.042
571 Ache, B. W., & Young, J. M. (2005). Olfaction: Diverse species, conserved principles.
572 *Neuron*, *48*(3), 417–430. https://doi.org/10.1016/j.neuron.2005.10.022
573 Almagro Armenteros, J. J., Tsirigos, K. D., Sønderby, C. K., Petersen, T. N., Winther,
574 O., Brunak, S., von Heijne, G., & Nielsen, H. (2019). SignalP 5.0 improves
575 signal peptide predictions using deep neural networks. *Nature Biotechnology*,
576 *37*(4), 420–423. https://doi.org/10.1038/s41587-019-0036-z
577 Altschul, S. F., Gish, W., Miller, W., Myers, E. W., & Lipman, D. J. (1990). Basic local
578 alignment search tool. *Journal of Molecular Biology*, *215*(3), 403–410.
579 https://doi.org/10.1016/s0022-2836(05)80360-2
580 Anson, L. C., Chen, P. E., Wyllie, D. J., Colquhoun, D., & Schoepfer, R. (1998).
581 Identification of amino acid residues of the NR2A subunit that control glutamate
582 potency in recombinant NR1/NR2A NMDA receptors. *The Journal of*
583 *Neuroscience*, *18*(2), 581–589.
584 Armstrong, N., Sun, Y., Chen, G.-Q., & Gouaux, E. (1998). Structure of a glutamate-
585 receptor ligand-binding core in complex with kainate. *Nature*, *395*(6705), 913–
586 917. https://doi.org/10.1038/27692
587 Baez, M. V., Cercato, M. C., & Jerusalinsky, D. A. (2018). NMDA receptor subunits
588 change after synaptic plasticity induction and learning and memory acquisition.
589 *Neural Plasticity*, *2018*, e5093048. https://doi.org/10.1155/2018/5093048
590 Bargmann, C. I. (2006). Comparative chemosensation from receptors to ecology.
591 *Nature*, *444*(7117), 295–301. https://doi.org/10.1038/nature05402

592 Benton, R., Vannice, K. S., Gomez-Diaz, C., & Vosshall, L. B. (2009). Variant
593 ionotropic glutamate receptors as chemosensory receptors in *Drosophila*. *Cell*,
594 *136*(1), 149–162. https://doi.org/10.1016/j.cell.2008.12.001
595 Cameron, J. L., & Fankboner, P. V. (1984). Tentacle structure and feeding processes
596 in life stages of the commercial sea cucumber *Parastichopus californicus*
597 (Stimpson). *Journal of Experimental Marine Biology and Ecology*, *81*(2), 193–
598 209. https://doi.org/10.1016/0022-0981(84)90006-6
599 Canario, A. V. M. (2021). *Transcriptomic tissue responses to pheromonal stimuli in*
600 Holothuria arguinensis. ArrayExpress database at EMBL-EBI. Experiment
601 ArrayExpress accession: E-MTAB-10369.
602 Chen, P. E., Johnston, A. R., Selina Mok, M., Schoepfer, R., & Wyllie, D. J. (2004).
603 Influence of a threonine residue in the S2 ligand binding domain in determining
604 agonist potency and deactivation rate of recombinant NR1a/NR2D NMDA
605 receptors. *The Journal of Physiology*, *558*(Pt 1), 45–58.
606 https://doi.org/10.1113/jphysiol.2004.063800
607 Collingridge, G. L., Olsen, R. W., Peters, J., & Spedding, M. (2009). A nomenclature
608 for ligand-gated ion channels. *Neuropharmacology*, *56*(1), 2–5.
609 https://doi.org/10.1016/j.neuropharm.2008.06.063
610 Corey, E. A., Bobkov, Y., Ukhanov, K., & Ache, B. W. (2013). Ionotropic crustacean
611 olfactory receptors. *PLoS One*, *8*(4), e60551.
612 https://doi.org/10.1371/journal.pone.0060551
613 Croset, V., Rytz, R., Cummins, S. F., Budd, A., Brawand, D., Kaessmann, H., Gibson,
614 T. J., & Benton, R. (2010). Ancient protostome origin of chemosensory
615 ionotropic glutamate receptors and the evolution of insect taste and olfaction.
616 *PLOS Genetics*, *6*(8), e1001064. https://doi.org/10.1371/journal.pgen.1001064

Díaz-Balzac, C. A., Abreu-Arbelo, J. E., & García-Arrarás, J. E. (2010). Neuroanatomy of the tube feet and tentacles in *Holothuria glaberrima* (Holothuroidea, Echinodermata). *Zoomorphology*, *129*(1), 33–43. https://doi.org/10.1007/s00435-009-0098-4

Díaz-Balzac, C. A., & García-Arrarás, J. E. (2018). Echinoderm Nervous System. In C. A. Díaz-Balzac & J. E. García-Arrarás, *Oxford Research Encyclopedia of Neuroscience*. Oxford University Press. https://doi.org/10.1093/acrefore/9780190264086.013.205

Giordano, G., Carbone, M., Ciavatta, M. L., Silvano, E., Gavagnin, M., Garson, M. J., Cheney, K. L., Mudianta, I. W., Russo, G. F., Villani, G., Magliozzi, L., Polese, G., Zidorn, C., Cutignano, A., Fontana, A., Ghiselin, M. T., & Mollo, E. (2017). Volatile secondary metabolites as aposematic olfactory signals and defensive weapons in aquatic environments. *Proceedings of the National Academy of Sciences*, *114*(13), 3451–3456. https://doi.org/10/f92sgq

González-Wangüemert, M., Valente, S., Henriques, F., Domínguez-Godino, J. A., & Serrão, E. A. (2016). Setting preliminary biometric baselines for new target sea cucumbers species of the NE Atlantic and Mediterranean fisheries. *Fisheries Research*, *179*, 57–66. https://doi.org/10.1016/j.fishres.2016.02.008

Grabherr, M., Hass, B. J., Yassour, M., Levin, J. Z., Thompson, D. A., Amit, I., Adiconis, X., Fan, L., Raychowdhury, R., Zeng, Q., Chen, Z., Mauceli, E., Hacohen, N., Gnirke, A., Rhind, N., di Palma, F., Birren, B. W., Nusbaum, C., Lindblad-Toh, K., … Regev, A. (2011). Full-length transcriptome assembly from RNA-Seq data without a reference genome. *Nature Biotechnology*, *29*, 644–652. https://doi.org/10.1038/nbt.1883

641 Groh-Lunow, K. C., Getahun, M. N., Grosse-Wilde, E., & Hansson, B. S. (2015).
642 Expression of ionotropic receptors in terrestrial hermit crab's olfactory sensory
643 neurons. *Frontiers in Cellular Neuroscience*, *8*, 448.
644 https://doi.org/10.3389/fncel.2014.00448
645 Guschanski, K., Warnefors, M., & Kaessmann, H. (2017). The evolution of duplicate
646 gene expression in mammalian organs. *Genome Research*, *27*(9), 1461–1474.
647 https://doi.org/10.1101/gr.215566.116
648 Haas, B. J., Papanicolaou, A., Yassour, M., Grabherr, M., Blood, P. D., Bowden, J.,
649 Couger, M. B., Eccles, D., Li, B., Lieber, M., MacManes, M. D., Ott, M., Orvis,
650 J., Pochet, N., Strozzi, F., Weeks, N., Westerman, R., William, T., Dewey, C.
651 N., … Regev, A. (2013). De novo transcript sequence reconstruction from RNA-
652 seq using the Trinity platform for reference generation and analysis. *Nature*
653 *Protocols*, *8*(8), 1494–1512. https://doi.org/10.1038/nprot.2013.084
654 Hall, M. R., Kocot, K. M., Baughman, K. W., Fernandez-Valverde, S. L., Gauthier, M.
655 E. A., Hatleberg, W. L., Krishnan, A., McDougall, C., Motti, C. A., Shoguchi, E.,
656 Wang, T., Xiang, X., Zhao, M., Bose, U., Shinzato, C., Hisata, K., Fujie, M.,
657 Kanda, M., Cummins, S. F., … Degnan, B. M. (2017). The crown-of-thorns
658 starfish genome as a guide for biocontrol of this coral reef pest. *Nature*,
659 *5*(544(7649)), 231–234. https://doi.org/10.1038/nature22033
660 Hamel, J.-F., & Mercier, A. (1996). Evidence of chemical communication during the
661 gametogenesis of holothuroids. *Ecology*, *77*(5), 1600–1616. Scopus.
662 https://doi.org/10.2307/2265555
663 Hamel, J.-F., & Mercier, A. (1999). Mucus as a mediator of gametogenic synchrony in
664 the sea cucumber *Cucumaria frondosa* (Holothuroidea: Echinodermata).

665 *Journal of the Marine Biological Association of the United Kingdom*, *79*(1), 121–
666 129. https://doi.org/10.1017/s0025315498000137
667 Hamel, J.-F., & Mercier, A. (2011). Diet and feeding behaviour of the sea cucumber
668 *Cucumaria frondosa* in the St. Lawrence estuary, eastern Canada. *Canadian*
669 *Journal of Zoology*. https://doi.org/10.1139/z98-040
670 Hansen, K. B., Yi, F., Perszyk, R. E., Menniti, F. S., & Traynelis, S. F. (2017). NMDA
671 Receptors in the Central Nervous System. In N. Burnashev & P. Szepetowski
672 (Eds.), *NMDA Receptors: Methods and Protocols* (pp. 1–80). Springer.
673 https://doi.org/10.1007/978-1-4939-7321-7_1
674 Hardege, J. D., & Bentley, M. G. (1997). Spawning synchrony in Arenicola marina:
675 Evidence for sex pheromonal control. *Proceedings of the Royal Society of*
676 *London. Series B: Biological Sciences*, *264*(1384), 1041–1047.
677 https://doi.org/10.1098/rspb.1997.0144
678 Hoekstra, L. A., Moroz, L. L., & Heyland, A. (2012). Novel insights into the echinoderm
679 nervous system from histaminergic and FMRFaminergic-like cells in the sea
680 cucumber *Leptosynapta clarki*. *PLoS ONE*, *7*(9), e44220.
681 https://doi.org/10.1371/journal.pone.0044220
682 Jin, R., Singh, S. K., Gu, S., Furukawa, H., Sobolevsky, A. I., Zhou, J., Jin, Y., &
683 Gouaux, E. (2009). Crystal structure and association behaviour of the GluR2
684 amino-terminal domain. *The EMBO Journal*, *28*(12), 1812–1823.
685 https://doi.org/10.1038/emboj.2009.140
686 Karakas, E., & Furukawa, H. (2014). Crystal structure of a heterotetrameric NMDA
687 receptor ion channel. *Science*, *344*(6187), 992–997.
688 https://doi.org/10.1126/science.1251915

689 Kaupp, U. B. (2010). Olfactory signalling in vertebrates and insects: Differences and
690 commonalities. *Nature Reviews Neuroscience*, *11*(3), 188–200.
691 https://doi.org/10.1038/nrn2789
692 Krogh, A., Larsson, B., von Heijne, G., & Sonnhammer, E. L. (2001). Predicting
693 transmembrane protein topology with a hidden Markov model: Application to
694 complete genomes. *Journal of Molecular Biology*, *305*(3), 567–580.
695 https://doi.org/10.1006/jmbi.2000.4315
696 Krueger, F. (2015). *'Trim galore' A wrapper tool around Cutadapt and FastQC to*
697 *consistently apply quality and adapter trimming to FastQ files*.
698 http://www.bioinformatics.babraham.ac.uk/projects/trim_galore/
699 Kumar, J., Schuck, P., & Mayer, M. L. (2011). Structure and assembly mechanism for
700 heteromeric kainate receptors. *Neuron*, *71*(2), 319–331.
701 https://doi.org/10.1016/j.neuron.2011.05.038
702 Lan, X., & Pritchard, J. K. (2016). Coregulation of tandem duplicate genes slows
703 evolution of subfunctionalization in mammals. *Science*, *352*(6288), 1009–1013.
704 https://doi.org/10.1126/science.aad8411
705 Langmead, B., & Salzberg, S. L. (2012). Fast gapped-read alignment with Bowtie 2.
706 *Nature Methods*, *9*(4), 357–359. https://doi.org/10.1038/nmeth.1923
707 Larsson, A. (2014). AliView: A fast and lightweight alignment viewer and editor for
708 large datasets. *Bioinformatics*, *30*(22), 3276–3278.
709 https://doi.org/10.1093/bioinformatics/btu531
710 Li, B., & Dewey, C. N. (2011). RSEM: Accurate transcript quantification from RNA-Seq
711 data with or without a reference genome. *BMC Bioinformatics*, *12*(1), 323.
712 https://doi.org/10.1186/1471-2105-12-323

713 Li, W., & Godzik, A. (2006). Cd-hit: A fast program for clustering and comparing large
714 sets of protein or nucleotide sequences. *Bioinformatics*, *22*(13), 1658–1659.
715 https://doi.org/10.1093/bioinformatics/btl158
716 Liang, D., Wang, T., Rotgans, B. A., McManus, D. P., & Cummins, S. F. (2016).
717 Ionotropic receptors identified within the tentacle of the freshwater snail
718 *Biomphalaria glabrata*, an intermediate host of *Schistosoma mansoni*. *PLOS*
719 *ONE*, *11*(6), e0156380. https://doi.org/10.1371/journal.pone.0156380
720 Liu, C., Pitts, R. J., Bohbot, J. D., Jones, P. L., Wang, G., & Zwiebel, L. J. (2010).
721 Distinct olfactory signaling mechanisms in the malaria vector mosquito
722 *Anopheles gambiae*. *PLoS Biology*, *8*(8).
723 https://doi.org/10.1371/journal.pbio.1000467
724 Marquet, N., Canário, A. V. M., & Power, D. M. (2020). Localization and distribution of
725 nitric oxide synthase and other neuronal markers in the podia of *Holothuria*
726 *arguinensis*. *Invertebrate Biology*, *139*(3). https://doi.org/10.1111/ivb.12298
727 Marquet, N., Cardoso, J. C. R., Louro, B., Fernandes, S. A., Silva, S. C., & Canario,
728 A. V. M. (2020). Holothurians have a reduced GPCR and odorant receptor-like
729 repertoire compared to other echinoderms. *Scientific Reports*, *10*(1), 3348.
730 https://doi.org/10.1038/s41598-020-60167-3
731 Marquet, N., Hubbard, P. C., Da Silva, J. P., Afonso, J., & Canário, A. V. M. (2018).
732 Chemicals released by male sea cucumber mediate aggregation and spawning
733 behaviours. *Scientific Reports*, *8*(1). https://doi.org/10.1038/s41598-017-
734 18655-6
735 Mayer, M. L., Ghosal, A., Dolman, N. P., & Jane, D. E. (2006). Crystal structures of
736 the kainate receptor GluR5 ligand binding core dimer with novel GluR5-

737 selective antagonists. *Journal of Neuroscience*, *26*(11), 2852–2861.
738 https://doi.org/10.1523/jneurosci.0123-06.2005
739 Miller, M. A., Pfeiffer, W., & Schwartz, T. (2010). Creating the CIPRES Science
740 Gateway for inference of large phylogenetic trees. *2010 Gateway Computing*
741 *Environments Workshop (GCE)*, 1–8.
742 https://doi.org/10.1109/gce.2010.5676129
743 Mistry, J., Chuguransky, S., Williams, L., Qureshi, M., Salazar, G. A., Sonnhammer,
744 E. L. L., Tosatto, S. C. E., Paladin, L., Raj, S., Richardson, L. J., Finn, R. D., &
745 Bateman, A. (2021). Pfam: The protein families database in 2021. *Nucleic Acids*
746 *Research*, *49*(D1), D412–D419. https://doi.org/10.1093/nar/gkaa913
747 Naur, P., Hansen, K. B., Kristensen, A. S., Dravid, S. M., Pickering, D. S., Olsen, L.,
748 Vestergaard, B., Egebjerg, J., Gajhede, M., Traynelis, S. F., & Kastrup, J. S.
749 (2007). Ionotropic glutamate-like receptor δ2 binds d-serine and glycine.
750 *Proceedings of the National Academy of Sciences*, *104*(35), 14116–14121.
751 https://doi.org/10.1073/pnas.0703718104
752 Ni, L., Klein, M., Svec, K. V., Budelli, G., Chang, E. C., Ferrer, A. J., Benton, R.,
753 Samuel, A. D., & Garrity, P. A. (2016). The ionotropic receptors IR21a and
754 IR25a mediate cool sensing in *Drosophila*. *ELife*, *5*, e13254.
755 https://doi.org/10.7554/elife.13254
756 Nicholas, K. B., & Nicholas, H. B. J. (1997). *GeneDoc: A tool for editing and annotating*
757 *multiple sequence alignments* (2.7.0) [Computer software].
758 https://github.com/karlnicholas/GeneDoc
759 Olivier, V., Monsempes, C., Francois, M. C., Poivet, E., & Jacquin-Joly, E. (2011).
760 Candidate chemosensory ionotropic receptors in a Lepidoptera. *Insect*

761 *Molecular Biology*, *20*(2), 189–199. https://doi.org/10.1111/j.1365-
762 2583.2010.01057.x
763 Pascual-Anaya, J., & D'Aniello, S. (2006). Free amino acids in the nervous system of
764 the amphioxus *Branchiostoma lanceolatum*. A comparative study. *International*
765 *Journal of Biological Sciences*, 87–92. https://doi.org/10.7150/ijbs.2.87
766 Purcell, S. W., Conand, C., Uthicke, S., & Byrne, M. (2016). Ecological roles of
767 exploited sea cucumbers. *Oceanography and Marine Biology: An Annual*
768 *Review*, *54*, 367–386. https://doi.org/10.1201/9781315368597-8
769 Raible, F., Tessmar-Raible, K., Arboleda, E., Kaller, T., Bork, P., Arendt, D., & Arnone,
770 M. I. (2006). Opsins and clusters of sensory G-protein-coupled receptors in the
771 sea urchin genome. *Developmental Biology*, *300*(1), 461–475.
772 https://doi.org/10.1016/j.ydbio.2006.08.070
773 Rambaut, A. (2016). *FigTree* (1.4.3) [Computer software].
774 https://github.com/rambaut/figtree/releases
775 Ramos-Vicente, D., Ji, J., Gratacòs-Batlle, E., Gou, G., Reig-Viader, R., Luís, J.,
776 Burguera, D., Navas-Perez, E., García-Fernández, J., Fuentes-Prior, P.,
777 Escriva, H., Roher, N., Soto, D., & Bayés, À. (2018). Metazoan evolution of
778 glutamate receptors reveals unreported phylogenetic groups and divergent
779 lineage-specific events. *ELife*, *7*, e35774. https://doi.org/10.7554/eLife.35774
780 Roberts, R. E., Motti, C. A., Baughman, K. W., Satoh, N., Hall, M. R., & Cummins, S.
781 F. (2017). Identification of putative olfactory G-protein coupled receptors in
782 crown-of-thorns starfish, *Acanthaster planci*. *BMC Genomics*, *18*(1), 400.
783 https://doi.org/10.1186/s12864-017-3793-4
784 Roberts, R. E., Powell, D., Wang, T., Hall, M. H., Motti, C. A., & Cummins, S. F. (2018).
785 Putative chemosensory receptors are differentially expressed in the sensory

786 organs of male and female crown-of-thorns starfish, *Acanthaster planci*. *BMC*
787 *Genomics*, *19*(1), 853. https://doi.org/10.1186/s12864-018-5246-0
788 Robinson, M. D., McCarthy, D. J., & Smyth, G. K. (2010). EdgeR: a Bioconductor
789 package for differential expression analysis of digital gene expression data.
790 *Bioinformatics*, *26*(1), 139–140. https://doi.org/10.1093/bioinformatics/btp616
791 Ronquist, F., Teslenko, M., van der Mark, P., Ayres, D. L., Darling, A., Höhna, S.,
792 Larget, B., Liu, L., Suchard, M. A., & Huelsenbeck, J. P. (2012). MrBayes 3.2:
793 Efficient bayesian phylogenetic inference and model choice across a large
794 model space. *Systematic Biology*, *61*(3), 539–542.
795 https://doi.org/10.1093/sysbio/sys029
796 Rytz, R., Croset, V., & Benton, R. (2013). Ionotropic Receptors (IRs): Chemosensory
797 ionotropic glutamate receptors in *Drosophila* and beyond. *Insect Biochemistry*
798 *and Molecular Biology*, *43*(9), 888–897.
799 https://doi.org/10.1016/j.ibmb.2013.02.007
800 San Miguel-Ruiz, J. E., Maldonado-Soto, A. R., & García-Arrarás, J. E. (2009).
801 Regeneration of the radial nerve cord in the sea cucumber *Holothuria*
802 *glaberrima*. *BMC Developmental Biology*, *9*, 3. https://doi.org/10.1186/1471-
803 213x-9-3
804 Sea Urchin Genome Sequencing, C., Sodergren, E., Weinstock, G. M., Davidson, E.
805 H., Cameron, R. A., Gibbs, R. A., Angerer, R. C., Angerer, L. M., Arnone, M. I.,
806 Burgess, D. R., Burke, R. D., Coffman, J. A., Dean, M., Elphick, M. R.,
807 Ettensohn, C. A., Foltz, K. R., Hamdoun, A., Hynes, R. O., Klein, W. H., …
808 Wright, R. (2006). The genome of the sea urchin *Strongylocentrotus*
809 *purpuratus*. *Science*, *314*(5801), 941–952.
810 https://doi.org/10.1126/science.1133609

811 Shepherd, J. D., & Huganir, R. L. (2007). The Cell Biology of Synaptic Plasticity: AMPA
812 Receptor Trafficking. *Annual Review of Cell and Developmental Biology*, *23*(1),
813 613–643. https://doi.org/10.1146/annurev.cellbio.23.090506.123516
814 Silbering, A. F., Rytz, R., Grosjean, Y., Abuin, L., Ramdya, P., Jefferis, G. S. X. E., &
815 Benton, R. (2011). Complementary function and integrated wiring of the
816 evolutionarily distinct *Drosophila* olfactory subsystems. *Journal of*
817 *Neuroscience*, *31*(38), 13357–13375. https://doi.org/10.1523/jneurosci.2360-
818 11.2011
819 Smith-Unna, R., Boursnell, C., Patro, R., Hibberd, J. M., & Kelly, S. (2016). TransRate:
820 Reference-free quality assessment of de novo transcriptome assemblies.
821 *Genome Research*, *26*(8), 1134–1144. https://doi.org/10.1101/gr.196469.115
822 Stamatakis, A. (2014). RAxML version 8: A tool for phylogenetic analysis and post-
823 analysis of large phylogenies. *Bioinformatics*, *30*(9), 1312–1313.
824 https://doi.org/10.1093/bioinformatics/btu033
825 Stepanyan, R., Hollins, B., Brock, S. E., & McClintock, T. S. (2004). Primary culture of
826 lobster (*Homarus americanus*) olfactory sensory neurons. *Chemical Senses*,
827 *29*(3), 179–187. https://doi.org/10.1093/chemse/bjh023
828 Stroebel, D., & Paoletti, P. (2020). Architecture and function of NMDA receptors: An
829 evolutionary perspective. *The Journal of Physiology*, *n/a*(n/a).
830 https://doi.org/10.1113/jp279028
831 Touhara, K., & Vosshall, L. B. (2009). Sensing odorants and pheromones with
832 chemosensory receptors. *Annual Review of Physiology*, *71*, 307–332.
833 https://doi.org/10.1146/annurev.physiol.010908.163209
834 Towns, J., Cockerill, T., Dahan, M., Foster, I., Gaither, K., Grimshaw, A., Hazlewood,
835 V., Lathrop, S., Lifka, D., Peterson, G. D., Roskies, R., Scott, J. R., & Wilkins-

Diehr, N. (2014). XSEDE: Accelerating scientific discovery. *Computing in Science & Engineering*, *16*(5), 62–74. https://doi.org/10.1109/mcse.2014.80

Traynelis, S. F., Wollmuth, L. P., McBain, C. J., Menniti, F. S., Vance, K. M., Ogden, K. K., Hansen, K. B., Yuan, H., Myers, S. J., & Dingledine, R. (2010). Glutamate receptor ion channels: Structure, regulation, and function. *Pharmacological Reviews*, *62*(3), 405–496. https://doi.org/10.1124/pr.109.002451

Tweedie, S., Braschi, B., Gray, K., Jones, T. E. M., Seal, R. L., Yates, B., & Bruford, E. A. (2021). Genenames.org: The HGNC and VGNC resources in 2021. *Nucleic Acids Research*, *49*(D1), D939–D946. https://doi.org/10.1093/nar/gkaa980

Twomey, E. C., & Sobolevsky, A. I. (2018). Structural mechanisms of gating in ionotropic glutamate receptors. *Biochemistry*, *57*(3), 267–276. https://doi.org/10.1021/acs.biochem.7b00891

Wudick, M. M., Michard, E., Oliveira Nunes, C., & Feijó, J. A. (2018). Comparing plant and animal glutamate receptors: Common traits but different fates? *Journal of Experimental Botany*, *69*(17), 4151–4163. https://doi.org/10.1093/jxb/ery153

Ye, J., Coulouris, G., Zaretskaya, I., Cutcutache, I., Rozen, S., & Madden, T. L. (2012). Primer-BLAST: A tool to design target-specific primers for polymerase chain reaction. *BMC Bioinformatics*, *13*(1), 134. https://doi.org/10.1186/1471-2105-13-134

Yelshanskaya, M. V., Li, M., & Sobolevsky, A. I. (2014). Structure of an agonist-bound ionotropic glutamate receptor. *Science*, *345*(6200), 1070–1074. https://doi.org/10.1126/science.1256508

859 Yohe, L. R., & Brand, P. (2018). Evolutionary ecology of chemosensation and its role
860 in sensory drive. *Current Zoology*, *64*(4), 525–533.
861 https://doi.org/10.1093/cz/zoy048
862

Figure legends:

Figure 1 - Dendrogram showing the number of putative iGluR subunits identified in the echinoderms. Homologues found in vertebrates (*H. sapiens* and *L. oculatus*) and in molluscs (*C. gigas* and *B. grablata*) are represented for comparison. The dendrogram represents the evolutionary relationship of the species and was manually designed having in consideration the tree of life web project (www.tolweb.org/tree) and the species taxonomic classification was based on http://www.marinespecies.org/. The unique echinoderm GluH subfamily is boxed. Accession numbers of all genes/transcripts are listed in Supplementary Table 2. * non-annotated genomes. + transcriptome, ni- not identified.

Figure 2 - The iGluR phylogenetic tree containing receptor subunits from echinoderms, molluscs, and vertebrates. The tree was built using the BI method and a similar tree with the ML methods is available as Supplementary Figure 1. Homologues from the plant *A. thaliana* (Ath_GLR2 NP_180476.3 and Ath_GLR7 NP_565744.1) were used as an outgroup. The same BI tree is represented in A and B. A) tree with collapsed receptor clusters and B) circular tree with all the species represented. In B) the posterior probability values and bootstrap replicates for the nodes that are supported by BI and ML trees are represented. The branches that include the representatives of the different echinoderm classes were coloured as well as the representatives of other phyla used in the analysis. * indicate the *A. planci* putative chemosensory iGluR (Roberts et al., 2017). Sequence abbreviations and accession numbers are listed in Supplementary Table 2. The sequence alignment used for tree building is available as Supplementary Data 1.

Figure 3 – Comparative schematic representation of the predicted protein domain organization of the echinoderm *H. arguinesis*, *A. japonicus* and *S. purpuratus* iGluR subunits. The consensus domain organization of *H. sapiens* GluA, GluK and GluD are represented on the top for comparison with the vertebrate model. The receptor linear structure represented was based on (Traynelis et al., 2010). Protein domains were either identified by querying the Pfam database or deduced from multiple sequence alignments with the vertebrate homologues and are represented by different colours: the amino-terminal domain (ATD, PF01094) is represented in pink; the ligand-binding

domain (S1 and S2 domains, PF10613 and PF00060, respectively) are marked with blue boxes, the three membrane-spanning helices (M1, M3, and M4) and a membrane re-entrant loop (M2)) of the transmembrane domains are represented in yellow and the C-terminal domains (CTD) in white. Homologue protein domains are represented by the same colours and the percent (%) amino acid sequence similarity between the echinoderm domains to the corresponding homologue region in *H. sapiens* and *L. oculatus* are indicated. The percent similarity of GluH domains was calculated against the vertebrate GluA and GluK homologue region. Only complete sequences were used with exception of the *A. japonicus* GluD which misses the N-terminus. The structural analysis of the individual echinoderm iGluR is available in Supplementary Figures 2, 3 and 4.

Figure 4 – Comparative sequence alignment of the predicted S1 and S2 motifs within the ligand-binding domain (LBD) of *H. arguinensis* (Har) and *A. japonicus* (Aja) with the *H. sapiens* (Hsa) iGluR subfamilies. The amino acids arginine (R, in blue) within the S1 domain and the threonine (T, in pink) and aspartic acid/glutamic acid (D/E, in green) within the S2 domain associated with G amino acid activation are coloured and marked in bold. Fully conserved amino acid positions are represented by "*", conservation between groups of strongly similar properties by ":" and conservation between groups of weakly similar properties with ".".

Figure 5 - Gene synteny of *A. japonicus Grih* subunit genome regions with other echinoderms (*S. purpuratus* and *A. planci*) and the vertebrate *L. oculatus*. Genes are represented by coloured boxes and their position in the genome assemblies is indicated in megabases (Mb). Neighbouring gene families are represented by different colours and homologue genes are indicated by the same colour. The *Grih* genes are indicated in red colour and the different receptor types are indicated inside the coloured box. The neighbouring genes of *A. japonicus* were used to identify gene homologues in the represented species. Neighbouring genes represented are: translin-associated protein X (*TSNAX*), TEF transcription factor member a (*TEFA*), matrix metalloproteinase-16 (MMP16), solute carrier family 3 member 1 (SLC3A1), SUB1 regulator of transcription (*SUB1*), gonadotropin releasing hormone receptor 2 (*GNRHR2*) , BCL2 Apoptosis Regulator (*BCL2*) , treslin-like (*TICRR*), sorbitol

dehydrogenase (*SORD*), FKBP prolyl isomerase (*fkbp8*), abhydrolase domain containing 17A, depalmitoylase (*abhd17aa*), solute carrier family 35 member F6 (*SLC35F6*). Accession numbers of the neighbouring genes is provided in Supplementary Table 3.

Figure 6 – Gene synteny of *A. japonicus* Grik genome regions with other echinoderms (*S. purpuratus* and *A. planci*) and vertebrates (*H. sapiens* and *L. oculatus*). Genes are represented by coloured boxes and their position in the genome assemblies is indicated in megabases (Mb). Neighbouring genes families are represented by different colours and homologue genes are indicated by the same colour. The Grik genes are indicated in red colour and the different receptor types are indicated inside the coloured box. Only genes that were common in all species are represented. The neighbouring genes of *A. japonicus* were used to identify gene homologues in the represented species. Neighbouring genes represented are: zinc finger containing ubiquitin peptidase 1 (*ZUP1*), centrosomal protein 162 (*CEP162*), retinoic acid induced 14 (*RAI14*), caseinolytic mitochondrial matrix peptidase chaperone subunit X (*CLPX*), programmed cell death 7 (*PDCD7*), damage specific DNA binding protein 1 cullin 4 (*DDB1-CUL4*), ankyrin repeat family A member 2 (*ANKRA2*), ribosomal protein S6 (*RPS6*), centrosomal protein 162 (*CE162*), elongin A (*ELOA*), betaine-homocysteine S-methyltransferase (*BHMT*), N-acetylated alpha-linked acidic dipeptidase 2 (*NAALAD2*), uracil phosphoribosyltransferase homolog (*UPRT*), ribosomal protein S4 X-linked (*RPS4X*). Accession numbers of the neighbouring genes is provided in Supplementary Table 2.

Figure 7 - Gene synteny of *A. japonicus Gria* and *Grid* genome regions with other echinoderms (*S. purpuratus* and *A. planci*) and the vertebrate *L. oculatus*. Genes are represented by coloured boxes and their position in the genome assemblies is indicated in megabases (Mb). Neighbouring genes families are represented by different colours and homologue genes are indicated by the same colour. Gria and Grid genes are indicated in red colour and the different receptor types are indicated inside the coloured box. Only genes common to all species are represented. The neighbouring genes of the *A. japonicus* were used to identify gene homologues in the

represented species. Neighbouring genes represented are: gamma-aminobutyric acid type A receptor subunit beta3 (*GABBR3*), gamma-aminobutyric acid type B receptor subunit 2 (*GABBR2*), phosphoglycerate kinase 1 (*PGK1*), F-box protein 39 (*FBXO39*), retinol dehydrogenase 13 (*RDH13*), somatomedin B and thrombospondin type 1 domain containing (*SBSPON*), corrinoid adenosyltransferase (*COBO*). Accession numbers of the neighbouring genes is provided in Supplementary Table 2.

Figure 8 - Expression levels (FPKM) of iGluR subunit transcripts in male and female *H. arguinensis*. Each tissue transcriptome was constructed from tissues collected from 12 males and 5 females. Different letters indicate significant differences between transcripts (sex, tissue and receptor). The level of significance is 5%.

Supplementary Table

Supplementary Table 1: Descriptive statistics of the de novo assembly transcriptomes from nerve ring (NR), radial nerve (RN) and tentacles (T).

Supplementary Table 2: List and accession numbers of iGluR subunits analysed in this study.

Supplementary Table 3: List of accession numbers, genome location and positions of the neighbouring genes used in the gene synteny analysis.

Supplementary Figures

Supplementary Figure 1: Phylogenetic tree of the *H. arguinesis* and *A. japonicus* and other vertebrate and invertebrate iGluRs. The tree was built using ML method.

Supplementary Figure 2: Schematic linear representation of the predicted structure of the *H. arguinensis* GluH subunits. The consensus structures of the *H. sapiens* GluA, GluK and GluD are represented for comparisons. Only complete sequences are represented with size indicated. The amino-terminal domain is represented in pink, the

ligand-binding domain (S1 and S2 domains) are marked with blue boxes, the transmembrane (TM) regions (the three membrane-spanning helices (M1, M3, and M4) and a membrane re-entrant loop (M2)) are represented in yellow and the C-terminal domains in indicated in white. The predicted signal peptide (SP) is also indicated.

Supplementary Figure 3: Schematic linear representation of the predicted structure of the iGluR subunit genes in *A. japonicus*. The consensus structures of the *H. sapiens* GluA, GluK and GluD is represented for comparisons. Only complete sequences are represented, and size (aa) is indicated. The amino-terminal domain is represented in pink, the ligand-binding domain (S1 and S2 domains) are marked with blue boxes, the transmembrane (TM) regions (the three membrane -spanning helices (M1, M3, and M4) and a membrane re-entrant loop (M2)) are represented in yellow and the C-terminal domains in indicated in white. The predicted signal peptide (SP) is also indicated.

Supplementary Figure 4: Schematic linear representation of the predicted structure of the iGluR subunit genes in *S. purpuratus*. The consensus structures of the *H. sapiens* GluA, GluK and GluD is represented for comparisons. Only complete sequences are represented, and size (aa) is indicated. The amino-terminal domain is represented in pink, the ligand-binding domain (S1 and S2 domains) are marked with blue boxes, the transmembrane (TM) regions (the three membrane-spanning helices (M1, M3, and M4) and a membrane re-entrant loop (M2)) are represented in yellow and the C -terminal domains in indicated in white. The predicted signal peptide (SP) is also indicated.

Supplementary Figure 5: Gene expression levels of *Griha5, Grihb, Grihc1* and *Grihc2* in nerve Ring (NR), radial nerve (RN) and tentacles (T) as determined by qPCR and normalized against *18s*, and represented as the mean ± SEM of three biological replicates (n= 3).

Supplementary Data

Supplementary Data 1: Aligned sequence alignment used to build the phylogenetic tree

Supplementary Data 2: Gene expression data set (tentacles, radial nerve and nerve ring) followed by three-way analysis of variance with sex, tissue and receptor subunit as factors to compare differences in expression levels (FPKM), followed by the multicomparison Holm-Sidak a posteriori test when main effects were statistically significant. Statistical analysis was performed using SigmaPlot software (version 14.0, Systat Software, Inc).

Table 1: Primer sequences, amplicon sizes and annealing temperatures (T) used in the qPCR analysis.

Transcript name	Fw/Rw	Primer sequence (5'−3')	Amplicon (bp)	T (°C)	E (%)	R^2
Harg_GluHA5	Fw	GCTCAGTACAACGACAGTAG	116	58	87.8	0.998
	Rv	TGTCATTCCCATGACTAGAAC				
Harg_GluHB	Fw	GGTCAGCCGAGTCAAGAACA	185	60	89.2	0.996
	Rv	GTGTAACGTAAGCCCTGCCT				
Harg_GluHC1	Fw	ACTTGAACCCACCGATCACC	120	60	90.7	0.997
	Rv	CTTCGACACTAGCCGAAATATA				
Harg_GluHC2	Fw	ATGCAGGTGGAAGAGGTATCC	189	60	91.1	0.998
	Rv	CCGCTTCACACTCCTCACAA				
18s	RT_F4	TGACGGAAGGGCACCACCAG	158	58	90.1	0.998
	RT_R4	AATCGCTCCACCAACTAAGAACGG				

Table 2: Nomenclature adopted to classify the ionotropic glutamate receptor subfamilies.

Subfamily	Gene/transcript	protein
AMPA	Gria	GluA
Kainate	Grik	GluK
NMDA	Grin	GluN
Delta	Grid	GluD
Echinoderm-specific	Grih	GluH

	GRIA (AMPA)	***GRIK*** (Kainate)	***GRID*** (Delta)	***GRIN*** (NMDA)	***GRIH*** (Echinoderm)	***GRIE*** (Epsilon)	***GRIF*** (Phi)	***IR*** (Ionotropic)	***TOTAL***
Homo sapiens	4	5	2	7	ni	ni	ni	ni	18
Lepisosteus oculatus	4	5	2	7	ni	ni	ni	ni	18
Branchiostoma lanceolatum	2	3	5	6	ni	4	2	ni	22
Anneissia japonica	1	2	1	2	2	2	ni	ni	10
Acanthaster planci	2	2	1	2	3	ni	ni	ni	10
Patiria miniata	2	1	1	2	3	ni	ni	ni	9
Asterias rubens	2	2	1	2	3	ni	ni	ni	10
Ophionereis fasciata *	ni	1	ni	ni	5	ni	ni	ni	6
Strongylocentrotus purpuratus	2	2	1	ni	5	ni	ni	ni	10
Lytechinus variegatus	3	2	1	ni	5	ni	ni	ni	11
Eucidaris tribuloides *	ni	4	1	ni	7	ni	ni	ni	13
Apostichopus japonicus	3	3	1	ni	11	ni	ni	ni	18
Holothuria arguinensis +	2	1	ni	ni	12	ni	ni	ni	15
Actinopyga echinites *	ni	ni	ni	ni	5	ni	ni	ni	5
Australostichopus mollis *	1	2	ni	ni	5	ni	ni	ni	8
Crassostrea gigas	3	3	3	5	ni	ni	ni	3	17
Biomphalaria glabrata	8	2	ni	4	ni	ni	ni	9	23

CHORDATA
VERTEBRATA
CEPHALOCHORDATA
ECHINODERMATA
AMBULACRARIA
CRINOIDEA
ASTROIDEA
OPHIUROIDEA
ECHINOIDEA
HOLOTUROIDEA
MOLLUSCA

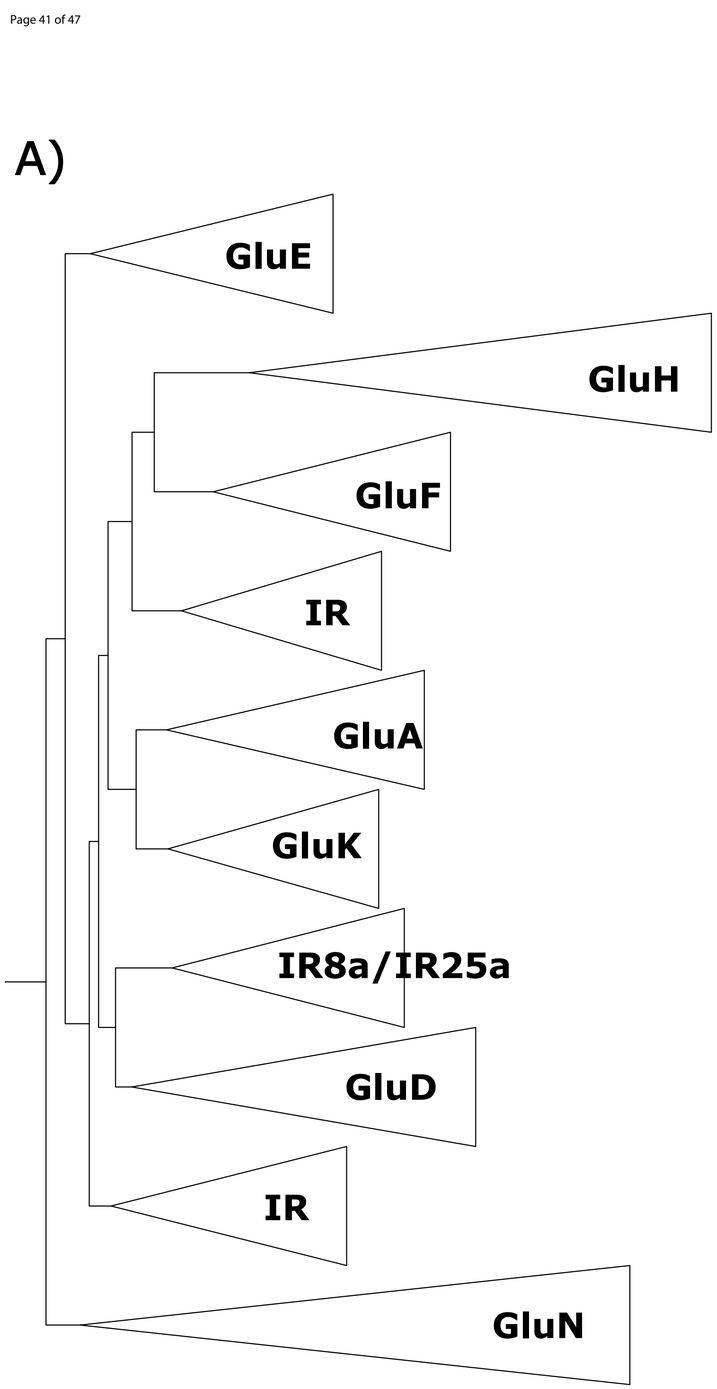
A)
GluE
GluH
GluF
IR
GluA
GluK
IR8a/IR25a
GluD
IR
GluN

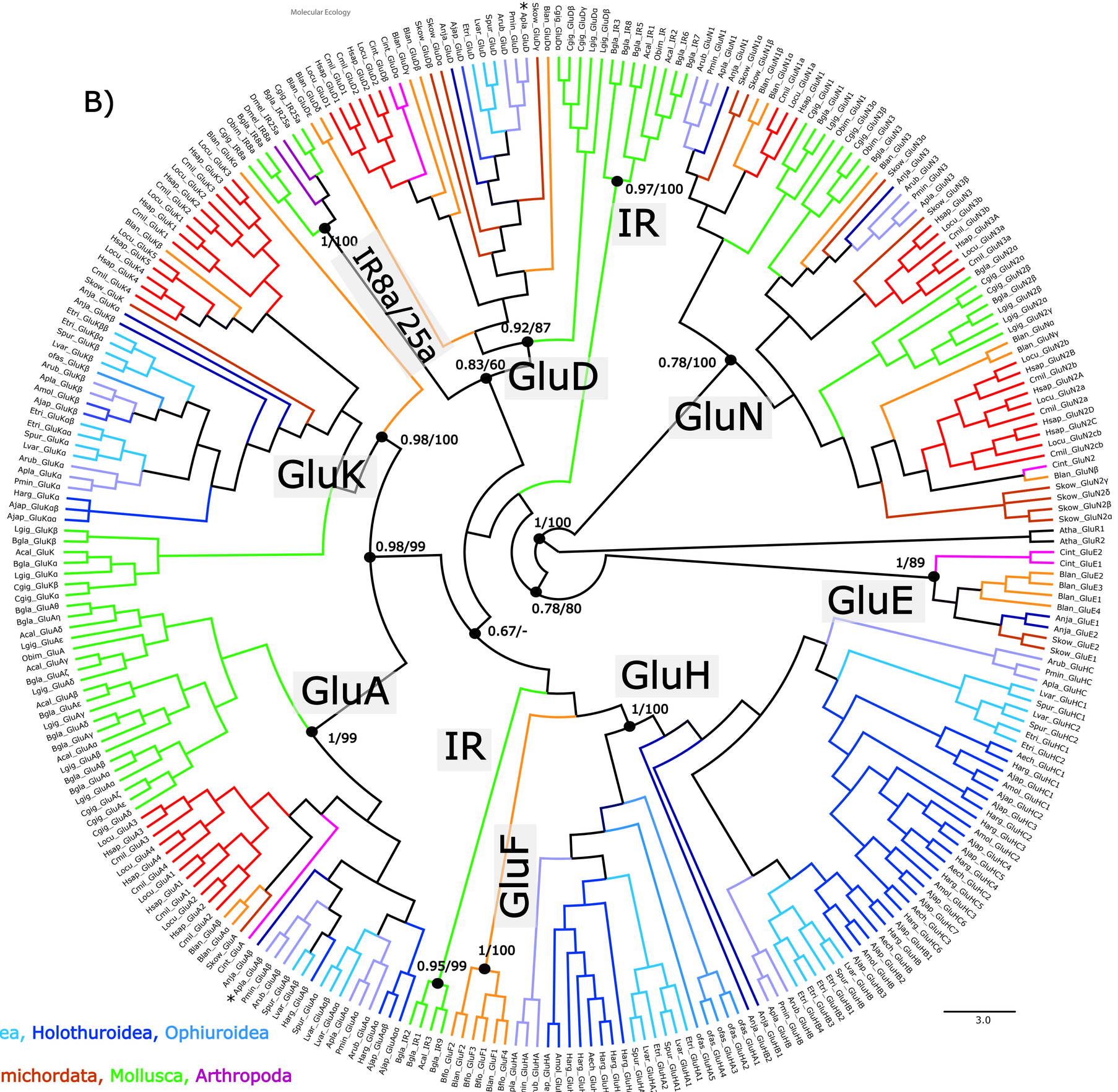
B)
IR8a/25a
GluK
GluD
IR
GluN
GluA
GluH
IR
GluF
GluE
1/100
0.97/100
0.92/87
0.83/60
0.78/100
0.98/100
0.98/99
1/100
0.78/80
0.67/-
1/89
1/99
1/100
0.95/99
1/100
3.0
Echinodermata classes: Astroidea, Crinoidea, Echinoidea, Holothuroidea, Ophiuroidea
Other phyla: Chordata, Cephalochordata, Tunicata, Hemichordata, Mollusca, Arthropoda

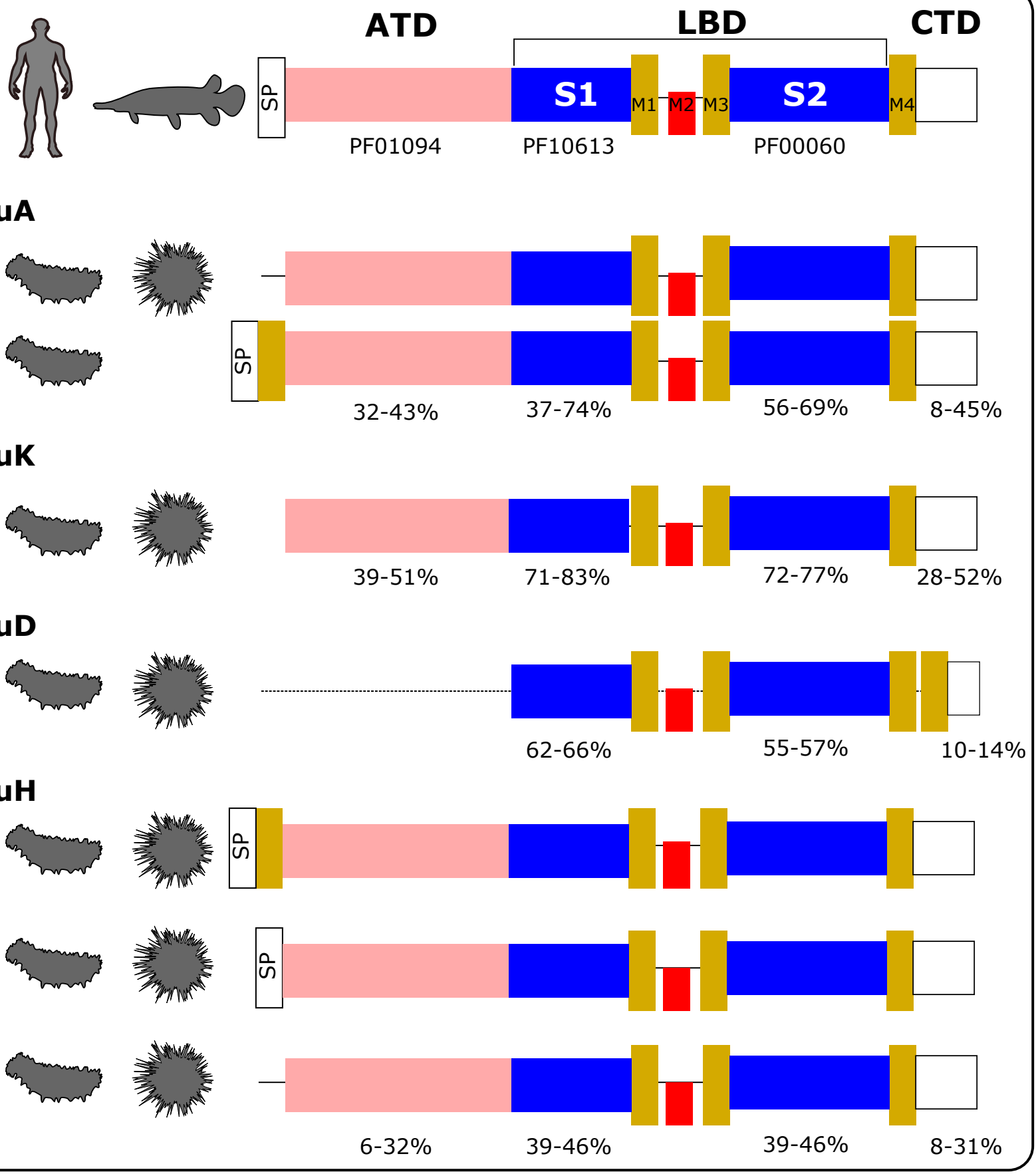
ATD
LBD
CTD
SP
S1
M1
M2
M3
S2
M4
PF01094
PF10613
PF00060
GluA
32-43%
37-74%
56-69%
8-45%
GluK
39-51%
71-83%
72-77%
28-52%
GluD
62-66%
55-57%
10-14%
GluH
6-32%
39-46%
39-46%
8-31%

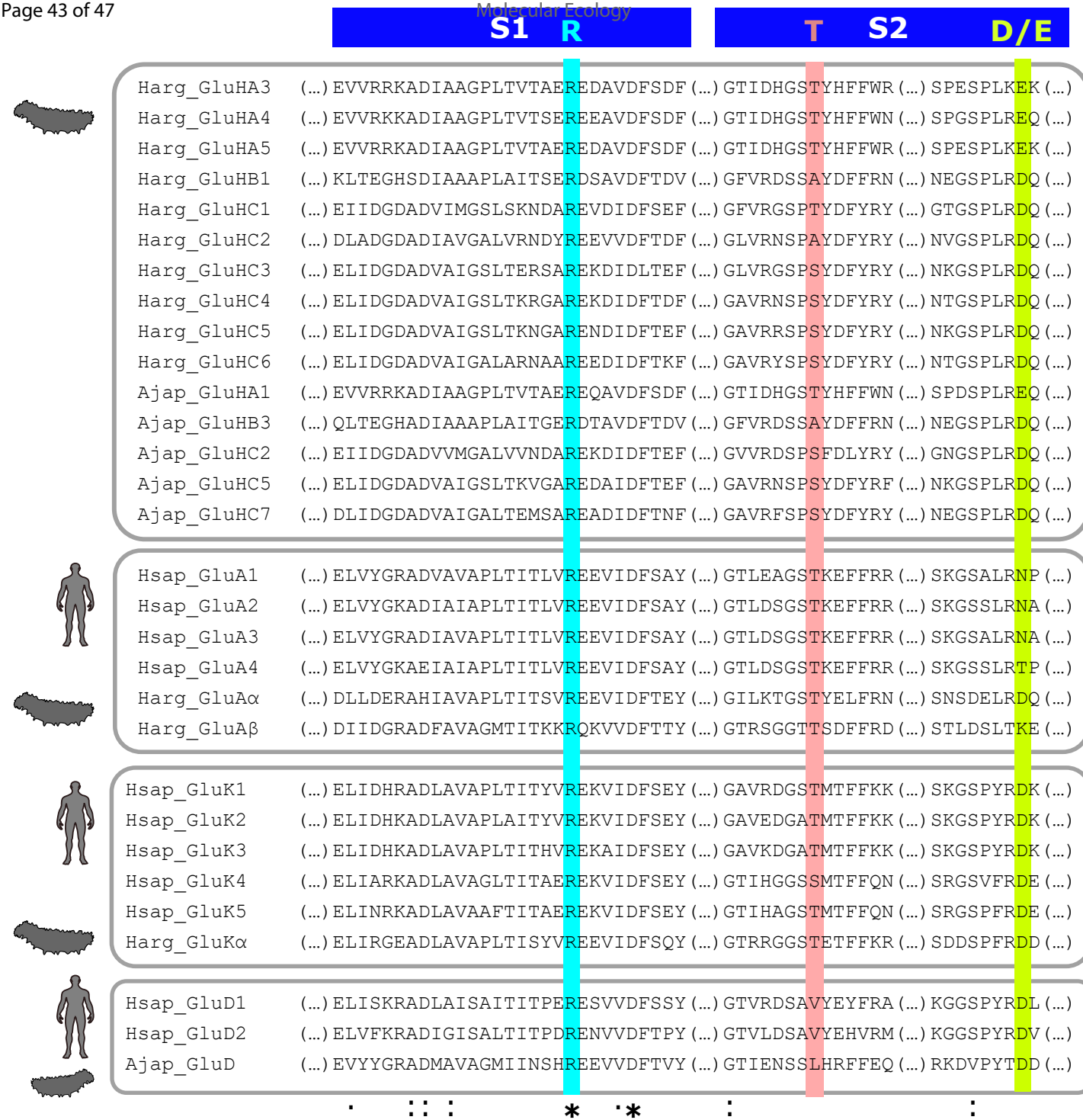
S1
R
T
S2
D/E
Harg_GluHA3 (…)EVVRRKADIAAGPLTVTAEREDAVDFSDF(…)GTIDHGSTYHFFWR(…)SPESPLKEK(…)
Harg_GluHA4 (…)EVVRKKADIAAGPLTVTSEREEAVDFSDF(…)GTIDHGSTYHFFWN(…)SPGSPLREQ(…)
Harg_GluHA5 (…)EVVRRKADIAAGPLTVTAEREDAVDFSDF(…)GTIDHGSTYHFFWR(…)SPESPLKEK(…)
Harg_GluHB1 (…)KLTEGHSDIAAAPLAITSERDSAVDFTDV(…)GFVRDSSAYDFFRN(…)NEGSPLRDQ(…)
Harg_GluHC1 (…)EIIDGDADVIMGSLSKNDAREVDIDFSEF(…)GFVRGSPTYDFYRY(…)GTGSPLRDQ(…)
Harg_GluHC2 (…)DLADGDADIAVGALVRNDYREEVVDFTDF(…)GLVRNSPAYDFYRY(…)NVGSPLRDQ(…)
Harg_GluHC3 (…)ELIDGDADVAIGSLTERSAREKDIDLTEF(…)GLVRGSPSYDFYRY(…)NKGSPLRDQ(…)
Harg_GluHC4 (…)ELIDGDADVAIGSLTKRGAREKDIDFTDF(…)GAVRNSPSYDFYRY(…)NTGSPLRDQ(…)
Harg_GluHC5 (…)ELIDGDADVAIGSLTKNGARENDIDFTEF(…)GAVRRSPSYDFYRY(…)NKGSPLRDQ(…)
Harg_GluHC6 (…)ELIDGDADVAIGALARNAAREEDIDFTKF(…)GAVRYSPSYDFYRY(…)NTGSPLRDQ(…)
Ajap_GluHA1 (…)EVVRRKADIAAGPLTVTAEREQAVDFSDF(…)GTIDHGSTYHFFWN(…)SPDSPLREQ(…)
Ajap_GluHB3 (…)QLTEGHADIAAAPLAITGERDTAVDFTDV(…)GFVRDSSAYDFFRN(…)NEGSPLRDQ(…)
Ajap_GluHC2 (…)EIIDGDADVVMGALVVNDAREKDIDFTEF(…)GVVRDSPSFDLYRY(…)GNGSPLRDQ(…)
Ajap_GluHC5 (…)ELIDGDADVAIGSLTKVGAREDAIDFTEF(…)GAVRNSPSYDFYRF(…)NKGSPLRDQ(…)
Ajap_GluHC7 (…)DLIDGDADVAIGALTEMSAREADIDFTNF(…)GAVRFSPSYDFYRY(…)NEGSPLRDQ(…)
Hsap_GluA1 (…)ELVYGRADVAVAPLTITLVREEVIDFSAY(…)GTLEAGSTKEFFRR(…)SKGSALRNP(…)
Hsap_GluA2 (…)ELVYGKADIAIAPLTITLVREEVIDFSAY(…)GTLDSGSTKEFFRR(…)SKGSSLRNA(…)
Hsap_GluA3 (…)ELVYGRADIAVAPLTITLVREEVIDFSAY(…)GTLDSGSTKEFFRR(…)SKGSALRNA(…)
Hsap_GluA4 (…)ELVYGKAEIAIAPLTITLVREEVIDFSAY(…)GTLDSGSTKEFFRR(…)SKGSSLRTP(…)
Harg_GluAα (…)DLLDERAHIAVAPLTITSVREEVIDFTEY(…)GILKTGSTYELFRN(…)SNSDELRDQ(…)
Harg_GluAβ (…)DIIDGRADFAVAGMTITKKRQKVVDFTTY(…)GTRSGGTTSDFFRD(…)STLDSLTKE(…)
Hsap_GluK1 (…)ELIDHRADLAVAPLTITYVREKVIDFSEY(…)GAVRDGSTMTFFKK(…)SKGSPYRDK(…)
Hsap_GluK2 (…)ELIDHKADLAVAPLAITYVREKVIDFSEY(…)GAVEDGATMTFFKK(…)SKGSPYRDK(…)
Hsap_GluK3 (…)ELIDHKADLAVAPLTITHVREKAIDFSEY(…)GAVKDGATMTFFKK(…)SKGSPYRDK(…)
Hsap_GluK4 (…)ELIARKADLAVAGLTITAEREKVIDFSEY(…)GTIHGGSSMTFFQN(…)SRGSVFRDE(…)
Hsap_GluK5 (…)ELINRKADLAVAAFTITAEREKVIDFSEY(…)GTIHAGSTMTFFQN(…)SRGSPFRDE(…)
Harg_GluKα (…)ELIRGEADLAVAPLTISYVREEVIDFSQY(…)GTRRGGSTETFFKR(…)SDDSPFRDD(…)
Hsap_GluD1 (…)ELISKRADLAISAITITPERESVVDFSSY(…)GTVRDSAVYEYFRA(…)KGGSPYRDL(…)
Hsap_GluD2 (…)ELVFKRADIGISALTITPDRENVVDFTPY(…)GTVLDSAVYEHVRM(…)KGGSPYRDV(…)
Ajap_GluD (…)EVYYGRADMAVAGMIINSHREEVVDFTVY(…)GTIENSSLHRFFEQ(…)RKDVPYTDD(…)

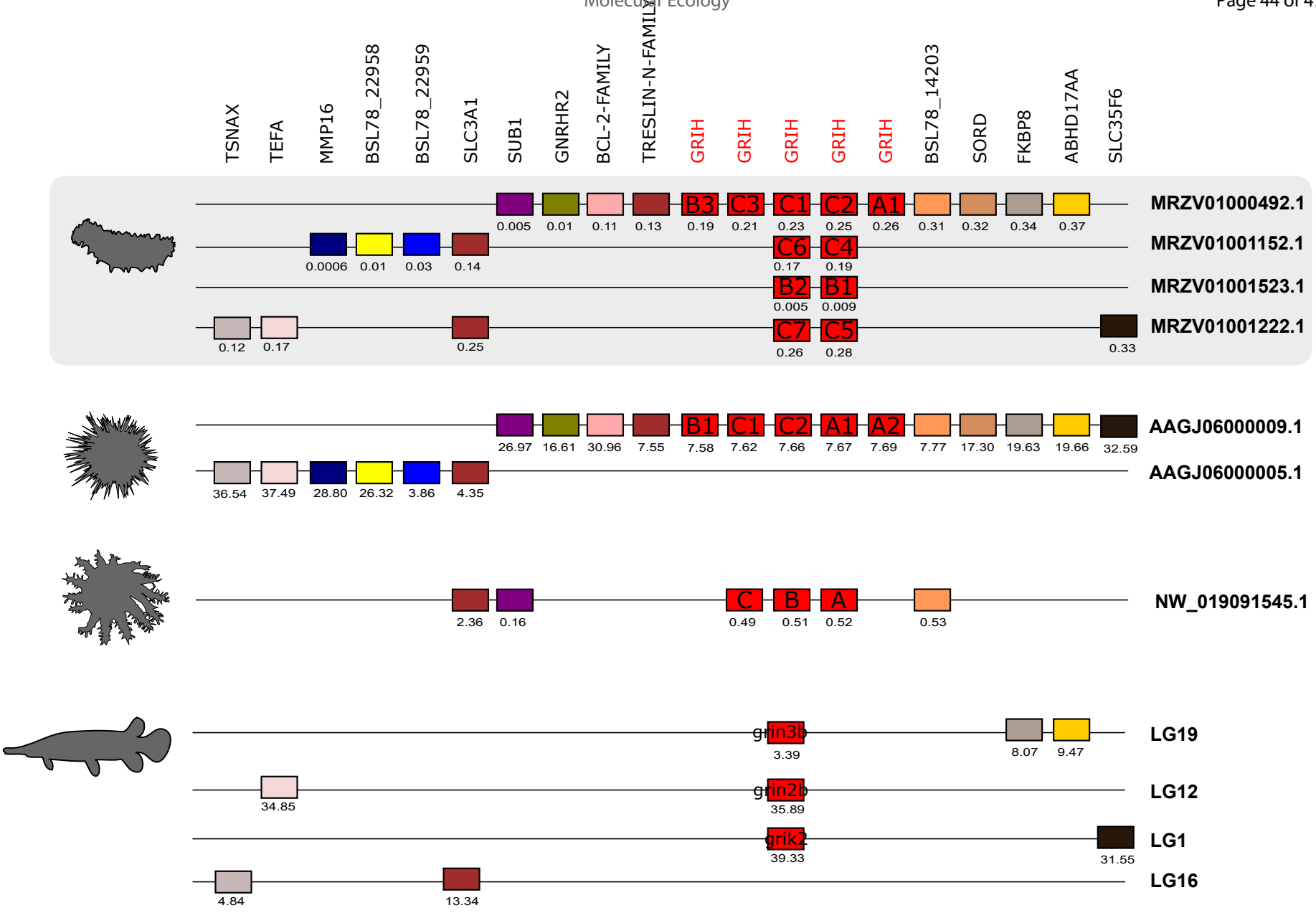
TSNAX
TEFA
MMP16
BSL78_22958
BSL78_22959
SLC3A1
SUB1
GNRHR2
BCL-2-FAMILY
TRESLIN-N-FAMILY
GRIH
GRIH
GRIH
GRIH
GRIH
BSL78_14203
SORD
FKBP8
ABHD17AA
SLC35F6
B3
C3
C1
C2
A1
0.005
0.01
0.11
0.13
0.19
0.21
0.23
0.25
0.26
0.31
0.32
0.34
0.37
MRZV01000492.1
0.0006
0.01
0.03
0.14
C6
C4
0.17
0.19
MRZV01001152.1
B2
B1
0.005
0.009
MRZV01001523.1
0.12
0.17
0.25
C7
C5
0.26
0.28
0.33
MRZV01001222.1
B1
C1
C2
A1
A2
26.97
16.61
30.96
7.55
7.58
7.62
7.66
7.67
7.69
7.77
17.30
19.63
19.66
32.59
AAGJ06000009.1
36.54
37.49
28.80
26.32
3.86
4.35
AAGJ06000005.1
2.36
0.16
C
B
A
0.49
0.51
0.52
0.53
NW_019091545.1
grin3b
3.39
8.07
9.47
LG19
34.85
grin2b
35.89
LG12
grik2
39.33
31.55
LG1
4.84
13.34
LG16

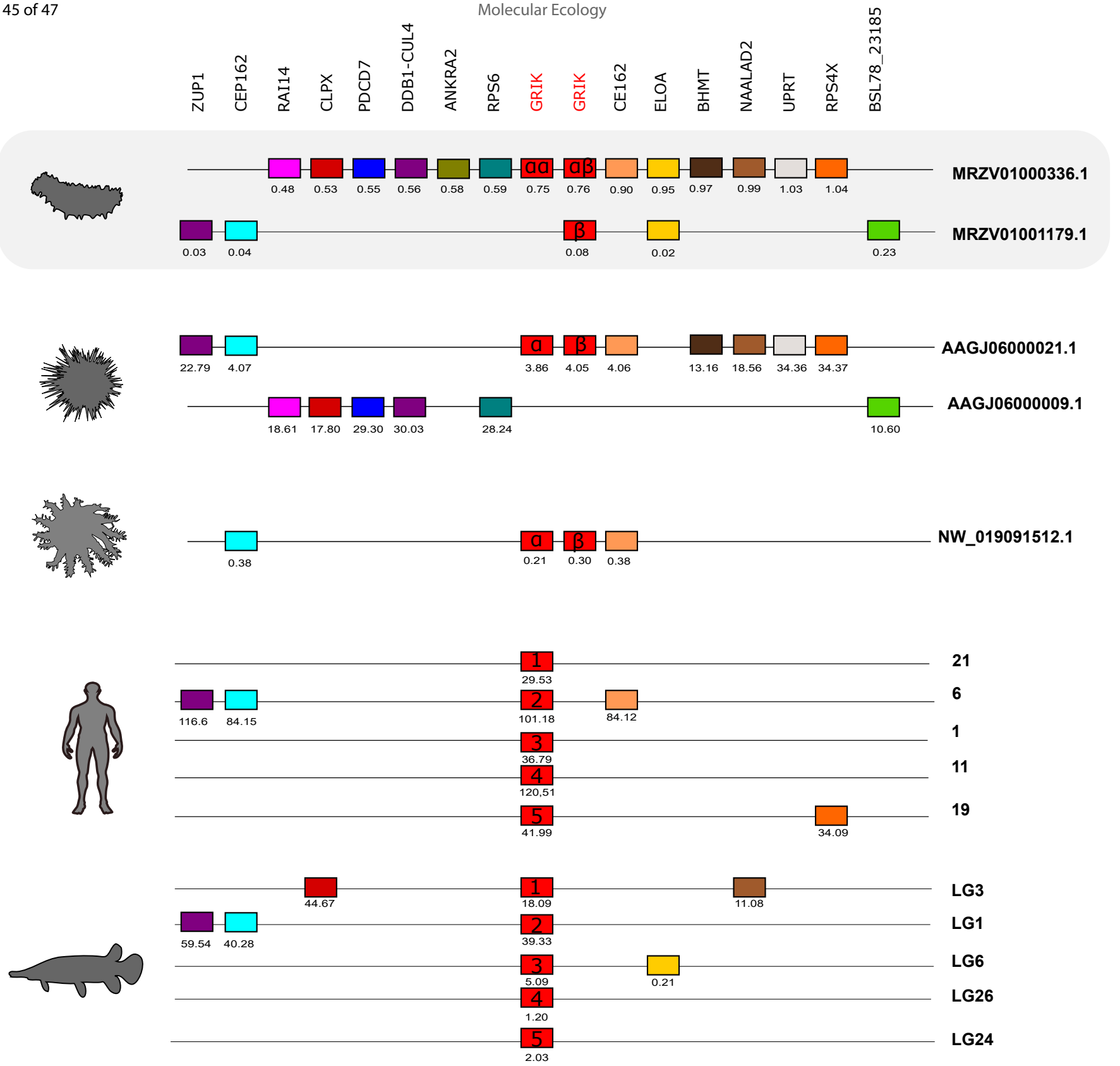
ZUP1
CEP162
RAI14
CLPX
PDCD7
DDB1-CUL4
ANKRA2
RPS6
GRIK
GRIK
CE162
ELOA
BHMT
NAALAD2
UPRT
RPS4X
BSL78_23185
αα
αβ
MRZV01000336.1
0.48 0.53 0.55 0.56 0.58 0.59 0.75 0.76 0.90 0.95 0.97 0.99 1.03 1.04
β
MRZV01001179.1
0.03 0.04 0.08 0.02 0.23
α β
AAGJ06000021.1
22.79 4.07 3.86 4.05 4.06 13.16 18.56 34.36 34.37
AAGJ06000009.1
18.61 17.80 29.30 30.03 28.24 10.60
α β
NW_019091512.1
0.38 0.21 0.30 0.38
1 2 3 4 5
21
6
1
11
19
29.53
116.6 84.15 101.18 84.12
36.79
120,51
41.99 34.09
LG3
LG1
LG6
LG26
LG24
44.67 18.09 11.08
59.54 40.28 39.33
5.09 0.21
1.20
2.03

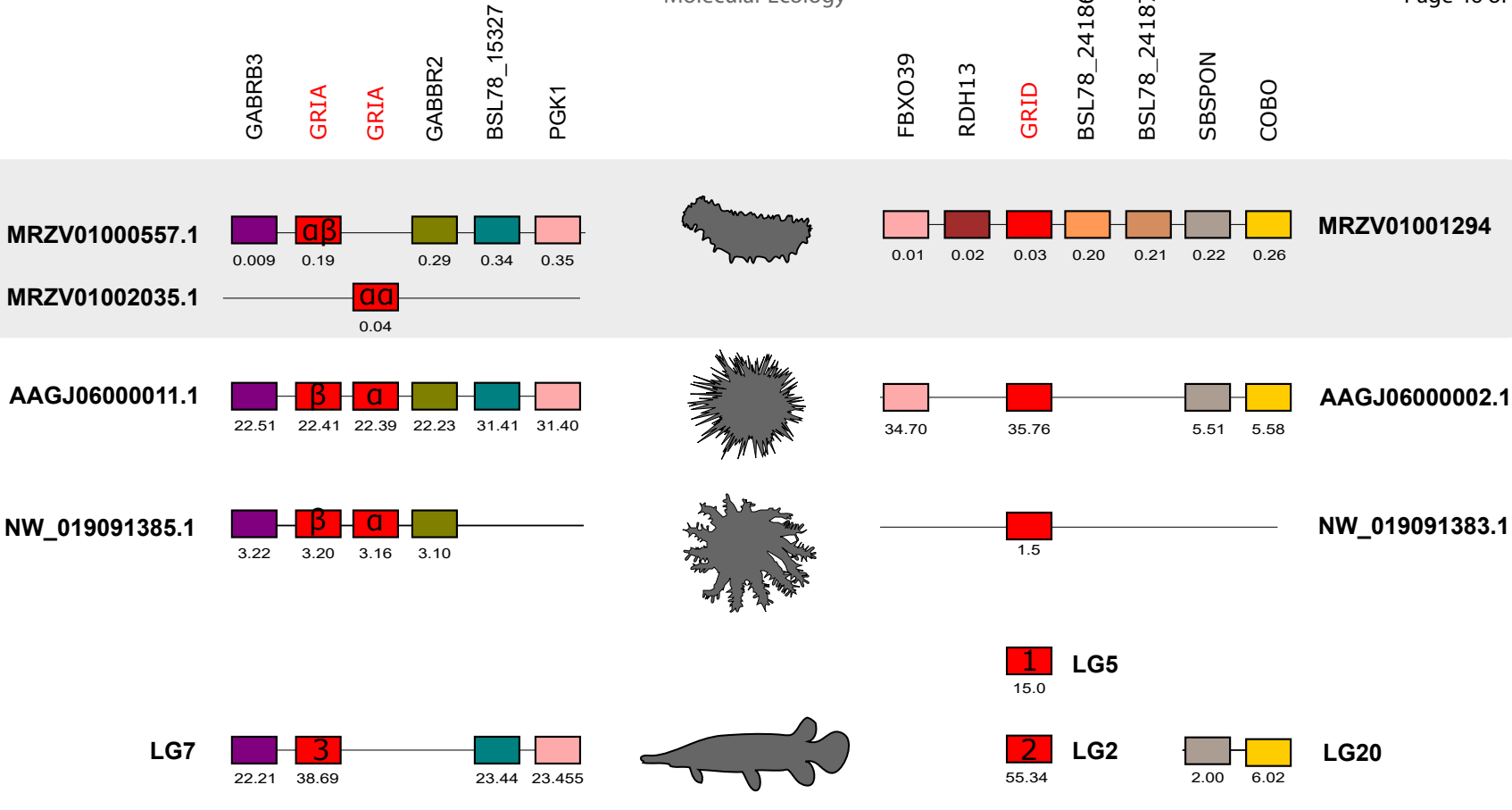
GABRB3
GRIA
GRIA
GABBR2
BSL78_15327
PGK1
FBXO39
RDH13
GRID
BSL78_24186
BSL78_24187
SBSPON
COBO
MRZV01000557.1
αβ
0.009
0.19
0.29
0.34
0.35
MRZV01002035.1
αα
0.04
0.01
0.02
0.03
0.20
0.21
0.22
0.26
MRZV01001294
AAGJ06000011.1
β
α
22.51
22.41
22.39
22.23
31.41
31.40
34.70
35.76
5.51
5.58
AAGJ06000002.1
NW_019091385.1
β
α
3.22
3.20
3.16
3.10
1.5
NW_019091383.1
1
15.0
LG5
LG7
3
22.21
38.69
23.44
23.455
2
55.34
LG2
2.00
6.02
LG20

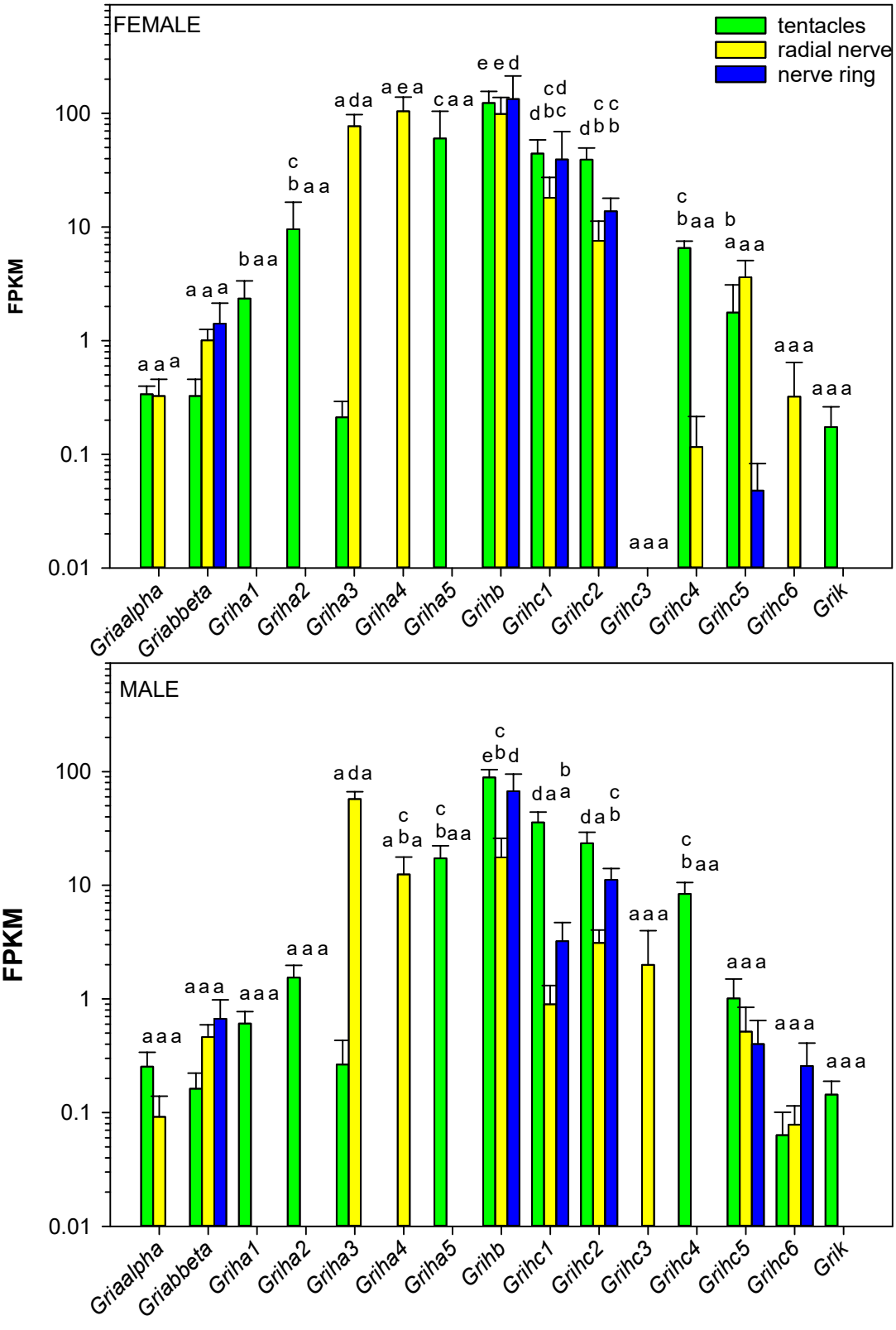
FEMALE
tentacles
radial nerve
nerve ring
FPKM
100
10
1
0.1
0.01
a a a
a a a
b a a
c b a a
a d a
a e a
c a a
e e d
c d d b c
c c d b b
a a a
c b a a
b a a a
a a a
a a a
Griaalpha
Griabbeta
Griha1
Griha2
Griha3
Griha4
Griha5
Grihb
Grihc1
Grihc2
Grihc3
Grihc4
Grihc5
Grihc6
Grik
MALE
FPKM
100
10
1
0.1
0.01
a a a
a a a
a a a
a a a
a d a
c a b a
c b a a
c e b d
b d a a
c d a b
a a a
c b a a
a a a
a a a
a a a
Griaalpha
Griabbeta
Griha1
Griha2
Griha3
Griha4
Griha5
Grihb
Grihc1
Grihc2
Grihc3
Grihc4
Grihc5
Grihc6
Grik